Title
Regulation of mitotic progression in Saccharomyces cerevisiae by the microtubule-associated proteins Slk19 and Stu1

Author
Faust, Ann Marie Elizabeth

Publication Date
2011

Peer reviewed|Thesis/dissertation

Regulation of mitotic progression in *Saccharomyces cerevisiae* by the microtubule-associated proteins Slk19 and Stu1

By

Ann Marie Elizabeth Faust

A dissertation submitted in partial satisfaction of the

requirements for the degree of

Doctor in Philosophy

in

Molecular and Cell Biology

in the

Graduate Division

of the

University of California, Berkeley

Committee in charge:

Professor Georjana Barnes, Chair
Professor W. Zacheus Cande
Professor Rebecca Heald
Professor Arash Komeili

Spring 2011

Abstract

Regulation of mitotic progression in *Saccharomyces cerevisiae* by the microtubule-associated proteins Slk19 and Stu1

By

Ann Marie Elizabeth Faust

Doctor of Philosophy in Molecular and Cell Biology

University of California, Berkeley

Professor Georjana Barnes, Chair

Mitosis is the process by which eukaryotic cells segregate their chromosomes before division. A critical stage of mitosis is anaphase, when the microtubule-based spindle segregates chromosomes into mother and daughter cells prior to cytokinesis. My dissertation research aimed to provide a better understanding of the regulation of anaphase progression and spindle function during mitosis in *Saccharomyces cerevisiae*.

My research focused on two microtubule-associated proteins, Slk19 (CENP-F homolog) and Stu1 (CLASP homolog). These proteins play fundamental roles in anaphase progression, Stu1 in microtubule spindle stability and Slk19 in spindle midzone organization and Cdc14 phosphatase regulation. I found that Stu1 and Slk19 physically interact and that Slk19 regulates Stu1 localization during anaphase. In addition to its interaction with Slk19, I identified a number of other physical and genetic interactors of Stu1 through mass spectrometry, yeast two-hybrid and synthetic genetic analyses. These interactors provide insight into the role of Stu1 at kinetochores. I also investigated Stu1 function through a protein truncation analysis and purification of full-length Stu1 protein. My truncation analysis revealed that the Stu1 C-terminus is dispensable for viability but is necessary for proper protein localization. The N-terminus, however, is essential for viability. My attempts to purify Stu1 from insect cells were partially successful; the protein is extremely sensitive to proteolytic degradation, and under conditions that limit proteolysis, the protein appears to aggregate or oligomerize in solution.

I also investigated the role of Slk19 sumoylation in anaphase progression. I determined that the Cdc14 early anaphase release (FEAR) network protein Slk19 is sumoylated in vivo and that sumoylation is important for restricting Cdc14 phosphatase localization to the nucleus at the end of anaphase. A *slk19* sumoylation mutant causes premature Cdc14 movement from the nucleus to the bud neck, which affects mitotic exit, as this *slk19* sumoylation mutant can partially rescue the spindle disassembly defect of the mitotic exit network mutant *cdc15-2*. This *slk19* mutant also has aberrant spindle elongation dynamics, which might be due to a change in Cdc14 function during anaphase. In conclusion, my dissertation research has uncovered a number of previously unrecognized interactions among mitotic proteins and has revealed a novel function of sumoylation in the regulation of Cdc14 function during anaphase through the FEAR network protein Slk19.

Dedication

This dissertation is dedicated to my husband, John, my father and mother, Chris and Laura, and my two sisters, Karen and Suzanne. My family has supported me unfailingly throughout my graduate studies and has always encouraged me to achieve my dream of earning a PhD.

Table of Contents

List of Figures

List of Tables

Acknowledgments

A PhD is not earned in a vacuum, and I would like to acknowledge the scientists and friends who have helped me along the way. First, I would like to acknowledge the support of my advisor, Georjana Barnes, and co-advisor, David Drubin. They are tirelessly supportive of their graduate students and have made their combined labs a collaborative and unique place to do scientific research. Next, I want to thank all of the present and former microtubule group members for countless discussions and helpful advice – Stefan Westermann, Yuko Nakajima, Jeffrey Woodruff, Connie Peng, Adrianne Pigula, Anthony Cormier, Nathaniel Krefman, Pantea Houshmand and Jonathan Wong. Outside of the microtubule group, I would especially like to acknowledge Christopher Toret, Brian Young, Voytek Okreglak, Yidi Sun and Susheela Carroll for making the lab a great place to work every day, even when the science was being difficult and the yeast weren't behaving. I would like to thank my collaborators for their contributions to my research projects: Sven Nelson in Stanley Fields' lab at the University of Washington and Anthony Hazbun at Purdue University for yeast 2-hybrid screens, Catherine Wong in John Yates' lab at Scripps Research Institute for mass spectrometric analyses, Charles Boone at the University of Toronto for sharing unpublished synthetic genetic array data with me, and Benjamin Montpetit in Karsten Weis' lab and Vincent Guacci in Douglas Koshland's lab at UC Berkeley for help with sumoylation detection. Finally, I want to thank my husband, John MacDonald, for following me to California when I know his heart is still in Boston, for sticking with me during my research education all these years and for sharing in my pain and my joy of scientific discovery. Without him, I could not have come this far.

Chapter 1: Introduction

1.1 Mitotic progression in eukaryotes

Mitosis is the process by which eukaryotic cells distribute their genetic material into two daughter cells. Before a cell divides, it must segregate identical populations of DNA into daughter cells. Chromosomal DNA must be segregated equally to ensure cell survival; consequently, cells use several mechanisms to ensure high-fidelity chromosomal segregation. While the details of these processes differ among organisms, the processes themselves are conserved in all eukaryotes. As my dissertation research strives to uncover details about some of these essential processes in *Saccharomyces cerevisiae*, I begin with a brief introduction to the key steps of yeast mitosis.

The division of nuclear DNA is accomplished by chromosomal segregation during the mitotic phase of the cell cycle. Duplicated DNA condenses to form identical, paired sister chromatids. These chromatids are distinct structures but are physically linked by cohesin proteins (Michaelis et al., 1997) and cannot be separated until the protease Separase (Esp1 in *S. cerevisiae*) cleaves the cohesins (Ciosk et al., 1998). Kinetochores, which are large proteinaceous structures, assemble on the centromeric DNA of sister chromatids (reviewed in Westermann et al., 2007). All of these steps must occur before chromatid segregation can proceed.

In budding yeast, the bipolar spindle is formed as the cell begins mitosis. The cell has two spindle pole bodies (yeast microtubule-organizing centers, analogous to centrosomes), and each member of a sister chromatid pair attaches, via kinetochore microtubules, to an opposite spindle pole. These microtubules, anchored at their minus ends to spindle poles, form attachments to kinetochores at their plus ends (Euteneuer and MacIntosh, 1981). In addition to kinetochore microtubules, cells possess another population of nuclear microtubules called interpolar microtubules. These microtubules are also anchored by their minus ends to spindle poles, but instead of attaching to kinetochores, they extend to the center of the spindle region and interact with interpolar microtubules from the opposite spindle pole (Winey and O'Toole, 2001). After the appropriate numbers of microtubules attach to each kinetochore (one in budding yeast, several in metazoans) and push the sister chromatids toward the center of the spindle, a spindle assembly checkpoint is relieved due to the correct formation of a bipolar spindle (reviewed in Musacchio and Hardwick, 2002). This phase constitutes metaphase; at this point, every sister chromatid is primed to move to its designated spindle pole. When the checkpoint is relieved, an anaphase-promoting protein complex (APC) is activated, which mediates cleavage of the cohesins that hold the sister chromatids together (Shirayama et al., 1999). After the sister chromatids are separated, the anaphase stage of mitosis begins.

Anaphase is characterized by two substages: anaphase A and anaphase B. The relative contributions to and timing of anaphase A and B in chromosome segregation vary among organisms, but they both must occur to ensure accurate segregation. In anaphase A, sister chromatids move to opposite spindle poles when the microtubules that are attached to their kinetochores depolymerize. This movement results in two identical populations of segregated DNA (Gorbsky et al., 1988; Winey and O'Toole, 2001). After the chromatids move to opposite poles, the entire spindle elongates in anaphase B to separate them

further. Interpolar microtubules polymerize and slide apart at the spindle midzone, resulting in the physical separation of the spindle poles (along with the attached sister chromatids) to the far edges of the mother and developing daughter cell (Gorbsky et al., 1988; Winey and O'Toole, 2001). At the end of anaphase, the spindle disassembles, a contractile ring forms between the two daughter cells as the mother cell undergoes cytokinesis.

While many of these processes are essential for cell survival, I am particularly interested in the events that occur during anaphase of mitosis. Specifically, I would like to understand the processes that are mediated by microtubule-associated proteins (MAPs) in budding yeast. Two major mechanisms of anaphase progression that involve MAPs are the maintenance of the spindle midzone and the regulation of mitotic proteins by post-translational modification. If the spindle forms incorrectly or disassembles before the end of mitosis, the chromosomes do not segregate properly, and cytokinesis may fail and/or aneuploidy may result. If the post-translational modifications of mitotic proteins are not properly spatiotemporally regulated, then mitotic progression may stall. There are major outstanding questions for these processes, detailed in the following chapters, which my dissertation research has explored in more detail.

1.2 The roles of microtubule-associated proteins at the spindle midzone

The spindle midzone is the small region of overlap of antiparallel microtubules emanating from opposite spindle poles. In budding yeast, this midzone region generally consists of 4-8 microtubules (Winey et al., 1995). A structure that is composed of so few microtubules is necessarily fragile and must be stabilized and tightly regulated to remain intact throughout anaphase. Because the spindle is crucial for chromosome segregation, there are many proteins and cellular mechanisms that help to ensure its integrity. The spindle midzone is not composed solely of microtubules; it also contains a number of MAPs (reviewed in Bouck and Bloom, 2005; Khmelinskii and Schiebel, 2008). There are five major functional classes of MAPs in budding yeast: kinesins and kinesin-like plus end-directed motor proteins, minus end-directed motors proteins, microtubule bundling proteins, plus-end binding proteins and plus-tip trackers, and chromosomal passenger proteins. Some MAPs span two or more of these categories, and all MAPs share the common property that they (directly or indirectly) bind to microtubules. The precise roles played by a particular MAP depend on its specific mechanism of interaction with microtubules and with other proteins. Many of the interactions among MAPs and effects that MAPs exert on microtubule dynamics and anaphase progression are unknown.

After SPBs duplicate, a short mitotic spindle forms between them, separating and pushing the SPBs to opposite ends of the nucleus. SPBs establish the proper microtubule orientation in mitosis, as the minus ends of microtubules must associate with the nuclear faces of SPBs and form an antiparallel structure. It has been shown that a number of MAPs contribute to the process of spindle establishment, including the plus end-directed kinesin motor proteins Cin8p and Kip1p (Hoyt et al., 1992), the minus end-directed motor protein Kar3p (Saunders et al., 1997) and the bundling protein Ase1p (Kotwaliwale et al., 2007).

The main function of the metaphase spindle is to help chromosomes congress to a central point between spindle poles. When each kinetochore microtubule has properly attached to a sister chromatid and the spindle checkpoint is relieved, anaphase A can begin. At this stage, kinetochore microtubules stop polymerizing and begin to depolymerize while still attached to kinetochores, pulling sister chromatids toward the spindle poles. While the details of this process are still under investigation, several MAPs that associate with the plus ends of kinetochore microtubules (e.g., the outer kinetochore Ndc80 complex (Wigge and Kilmartin, 2001; Wei et al., 2005; Wei et al., 2007), the plus end binding protein Stu2p (Tanaka et al., 2005), the Ipl1 kinase complex (Aurora B in metazoans) (Biggins and Murray, 2001; Tanaka et al., 2002), and the Dam1 ring complex (Westermann et al., 2005)) help to maintain the connection between the microtubule and the kinetochore.

During anaphase B, microtubules perform a very different spindle function to move the two populations of separated sister chromatids to opposite ends of the cell. The interpolar microtubules (rather than the kinetochore microtubules) push the chromatids apart. Interpolar microtubules are anchored at their minus ends to the spindle poles and extend toward the opposite spindle pole, ending at approximately half the distance to the opposite pole. The plus ends of interpolar microtubules associate at the center of the spindle, creating a zone of antiparallel interactions called the midzone (Winey et al., 1995). The antiparallel organization of microtubules creates a framework for MAPs to associate with and strengthen the spindle (reviewed in Khmelinskii and Schiebel, 2008).

Once the spindle midzone has formed, the microtubule plus ends at the midzone can polymerize to lengthen the spindle and push the spindle poles and sister chromatids apart (known as anaphase B). MAPs also help to provide the pushing force necessary to elongate the spindle as microtubules polymerize at the midzone. MAPs provide resistive and anchoring forces against polymerizing microtubules; as microtubules add subunits, those subunits are forced toward the center of the spindle, leading to a net increase in spindle length. To elongate the spindle, the plus end-directed kinesins Cin8 and Kip1 attach to antiparallel microtubules at the spindle midzone and "walk" toward the microtubule plus end, pushing microtubules away from each other (Saunders et al., 1995). The bundling protein Ase1 binds to antiparallel microtubules and helps to bundle them during anaphase B (Schuyler et al., 2003). This activity is necessary because if microtubules separate from each other too quickly, the spindle breaks down at the midzone, and chromatids are unable to separate properly.

While all stages of mitotic spindle assembly and development involve numerous MAPs, the structure of the spindle midzone during anaphase B elongation has the most critical need for MAP involvement. The midzone is a transient, dynamic structure that is composed of antiparallel interpolar microtubules and a variety of MAPs. Spindle microtubules undergo polymerization, depolymerization and sliding activities that are regulated by MAPs. If the spindle breaks or disassembles prematurely at the midzone, chromosomes fail to segregate, resulting in genomic instability and cell death. The stability of the midzone is enhanced by numerous MAPs and MAP complexes with unique but partially overlapping roles in maintaining stability throughout anaphase. At the point at which the spindle begins to elongate in anaphase B, a number of MAPs undergo spatial reorganization to associate with the midzone. The Ipl1 kinase complex helps to correct improper kinetochore-microtubule attachments prior to anaphase A but moves from kinetochores to the spindle midzone after proper attachments have been made (Chan and Botstein, 1993; Kim et al., 1999; Sandall et al., 2006; Nakajima et al., 2009). This movement is dependent on the dephosphorylation of Sli15p by the phosphatase Cdc14p (Pereira and Schiebel, 2003). The Esp1p/Slk19p complex (Esp1p is also known as separase) also moves from the kinetochore to the spindle midzone after Esp1p is activated by the Anaphase-Promoting Complex/Cyclosome (APC/C) and cleaves the cohesins that hold the sister chromatids together (Sullivan et al., 2001). The CBF3 kinetochore complex (Ndc10, Ctf13, Cep3 and Skp1) moves from its pre-anaphase inner kinetochore location (the interface between centromeric DNA and proteins of the kinetochore structure) to the spindle midzone upon APC/C activation (Bouck and Bloom, 2005). Stu1, which is associated with kinetochores and the short pre-anaphase spindle during metaphase, becomes focused entirely at the spindle midzone during anaphase B (Yin et al., 2002). While we know that these proteins move to the spindle at specific times, we do not understand most of the signals that prompt these movements or many of the activities that they perform at the midzone.

The spindle midzone must be organized in a way that allows proper spindle elongation. Recent evidence has shown that the MAP Ase1 forms at least part of the foundation of the midzone. Ase1 (PRC1 in metazoans) is a microtubule-bundling protein; as a homotetramer, it is thought to hold antiparallel microtubules together at the midzone (Schuyler et al., 2003). Ase1 must localize to the midzone before a number of other MAPs may associate there (Khmelinskii et al., 2007). The reason why it must localize to the

midzone before other MAPs is unclear. Spindle midzone organization cannot be solely dependent on Ase1, because yeast *ase1Δ* mutants can still form spindles and complete mitosis, albeit less efficiently than wild type cells (Schuyler et al., 2003). After Ase1 localizes to the spindle midzone, several other MAPs, including Stu1, Bim1, Bik1, Cin8 and Kip3, are able to localize there (Khmelinskii et al., 2007). Plus end-directed motor proteins such as Cin8 are essential for proper spindle elongation because they are thought to function as molecular "ratchets," allowing microtubules to slide against each other in one direction (so their plus ends move closer together) but suppressing movement in the opposite direction, preventing spindle shortening (Cordova et al., 1992; reviewed in Wu et al., 2006).

Spindle elongation from the midzone depends on microtubule polymerization at the plus ends in addition to antiparallel microtubule bundling and plus end-directed motor activities. While microtubule polymerization can occur spontaneously under certain conditions, several MAPs are thought to regulate polymerization at the midzone during spindle elongation. In yeast, homologs of XMAP215 and CLASP proteins (Stu2 and Stu1, respectively, in budding yeast) are the primary candidates for regulators of microtubule plus end polymerization (reviewed in Slep, 2009). The current model is that these proteins, by way of their HEAT- (Huntingtin, Elongation factor 3, PR65/A subunit of protein phosphatase A, TOR; made up of two antiparallel α-helices) and TOG- (Tumor Over-expressed Gene; made up of a number of HEAT repeats) containing domains, bind to individual tubulin dimers and deliver them to the plus end through their affinities for the plus end; these deliveries serve to promote polymerization (in the case of XMAP215) or rescue catastrophe events (in the case of CLASP) (Andrade et al., 2001; Okhura et al., 2001; Al-Bassam et al., 2006, Brouhard et al., 2008; Al-Bassam et al., 2010). These mechanisms of MAP modulation of microtubule dynamics at the midzone, together with the bundling, motor and signaling activities of other MAPs, allow the coordinated elongation of the spindle until the end of anaphase.

There are a number of outstanding questions in our understanding of the events occurring at the spindle midzone. It is unclear how the proteins located at the midzone are assembled at the midzone, the order in which they are assembled, and the signals that direct them to move to the midzone. Furthermore, the relative contributions of antiparallel microtubule bundling, microtubule binding, kinesin activity and modulation of microtubule dynamics to proper midzone function are not known. Investigation of the MAPs that are essential for viability, including Stu1, will be useful in understanding the minimal requirements for a functional spindle midzone.

1.3 Regulation of mitotic proteins by post-translational modification

The activities of a number of kinases and phosphatases regulate anaphase progression in interrelated ways. The major regulatory kinase during mitosis in *S. cerevisiae* is Cdc28 (cyclin-dependent kinase 1, CDK1), but a number of other kinases, including Cdc5 (Polo-like kinase), Ipl1 (Aurora B kinase) and the spindle assembly checkpoint kinases Bub1 and Mps1, play important roles during this stage of mitosis. Because phosphorylation must be tightly controlled in space and time, a number of phosphatases, including Cdc14, Cdc55 (PP2A in metazoans) and Glc7 (PP1 in metazoans), are also crucial for mitotic progression (reviewed in De Wulf et al., 2009).

Prior to anaphase onset, proteins involved in the spindle assembly checkpoint are regulated by the kinases Bub1 and Mps1. Bub1 has been shown to phosphorylate the histone H2A in *S. pombe* (Kawashima et al., 2010), but phosphorylation targets have not been identified in budding yeast. Human Bub1, however, has been shown to phosphorylate the anaphase-promoting complex regulator Cdc20 (Tang et al., 2004). Budding yeast Mps1 phosphorylates itself, the spindle assembly checkpoint protein Mad1 and the MAPs Ndc80 and Dam1 (Lauze et al., 1995; Hardwick et al., 1996; Kemmler et al., 2009; Shimogawa et al., 2006). The reasons for these kinase activities are unclear, but they might be important for protein-protein interactions or the formation of a checkpoint "scaffold" structure at kinetochores (reviewed in Zich and Hardwick, 2010). The Ipl1 kinase complex is also active at this stage, as Ipl1 phosphorylation of the MAPs Dam1 and Ndc80 is thought to destabilize inappropriate kinetochore-microtubule attachments (Kang et al., 2001; Akiyoshi et al., 2009).

At anaphase onset, Cdc28 kinase activity is high, partially due to the sequestration and functional inactivation of Cdc14 phosphatase. Proteins such as Ase1, Sli15 and Fin1 must be initially phosphorylated by Cdc28 for their proper function (Khmelinskii et al., 2009; Pereira and Schiebel, 2003; Woodbury and Morgan, 2007). The balance between phosphorylation by Cdc28 and dephosphorylation by Cdc14 is finely tuned during anaphase, as these same Cdc28 substrates must be dephosphorylated by Cdc14 in a temporally restricted manner (Pereira and Schiebel, 2003; Woodbury and Morgan, 2007; Jin et al., 2008; Khmelinskii et al., 2009). At the end of anaphase, the balance shifts toward dephosphorylation by Cdc14 due to the combination of full release of Cdc14 from the nucleolus to the nucleus and then to the cytoplasm (Visintin et al., 1998; Stegmeier and Amon, 2002) and the degradation of the cyclin binding partners of Cdc28 (Visintin et al., 1998). This shift toward dephosphorylation of target substrates is important for the continued stability of the spindle as it reaches its maximum length, just prior to disassembly and mitotic exit (Khmelinskii et al., 2007).

In contrast to phosphorylation, peptide modifications such as ubiquitination, neddylation and sumoylation are unique in that they covalently link small protein modifiers (ubiquitin, nedd and SUMO, respectively) to their targeted protein substrates. They are responsible for a number of changes in protein stability and function (reviewed in Liu and Walters, 2010; Xirodimas, 2008; Gareau and Lima, 2010). In particular, sumoylation has been shown to play important and varied roles in mitosis (Dieckhoff et al., 2004; reviewed in Dasso, 2008).

The small protein SUMO (Small Ubiquitin-Like Modifier), encoded by the *SMT3* gene in budding yeast, is a 101-a.a. protein that is conjugated to substrate lysines following a

loose consensus sequence on the substrate ([ILV][K][X][DE], Bernier-Villamor et al., 2002; Yunus and Lima, 2006). Like ubiquitination, its conjugation to substrates is dependent on the processing enzymes that make up the SUMO conjugation pathway (reviewed in Gareau and Lima, 2010). In budding yeast, there are two SUMO-activating enzymes, Aos1-Uba2 (analogous to E1 enzymes in the ubiquitin pathway), one SUMO conjugating enzyme, Ubc9p (E2) and at least four SUMO ligases, Siz1p, Siz2p/Nfi1p, Zip3p and Mms21p (E3s). Sumoylation is a dynamic process, however, with many substrates being sumoylated only transiently; thus, SUMO also has specific proteases. In budding yeast, SUMO can be cleaved from its substrates by the SUMO proteases Ulp1p and Ulp2p (Li and Hochstrasser, 2000, 2003). Both sumoylation and desumoylation are essential processes in yeast, highlighting the importance of this posttranslational modification as well as the importance of its temporal and spatial regulation.

The roles of sumoylation in mitotic regulation represent an increasingly important topic of study. In an early study of sumoylation, it was found that the budding yeast SUMO-conjugating enzyme Ubc9p is essential for cyclin degradation (Seufert et al., 1995). Another study cloned the gene encoding human SUMO*, HSMT3*, based on the yeast *SMT3* gene that was found in a screen for suppressors of *MIF2* mutants that caused defects in chromosome segregation (Mannen et al., 1996). More recently, several studies have identified mitotically active yeast proteins that are sumoylated and that this sumoylation aids in the regulation of their functions. The microtubule and/or kinetochore-associated proteins Ndc80p, Bir1p, Mif2p, Ndc10 and Kar9p are sumoylated, and the loss of sumoylation of these proteins leads to mitotic defects (Montpetit et al., 2006; Leisner et al., 2008). The metazoan mitotic proteins Hec1, Cenp-C, Survivin and Topoisomerase II have been shown to be sumoylated as well (reviewed in Dasso, 2008). These studies have shown that sumoylation is involved in many mitotic processes and may be part of the overall regulatory mechanism of mitotic progression, similar to the mechanisms found for protein phosphorylation.

The study of sumoylation and its role in mitosis, however, has been complicated by the fact that transient sumoylation of target substrates is difficult to detect. A number of large-scale yeast protein sumoylation screens have been undertaken (Zhou et al., 2004; Wohlschlegel et al., 2004; Wykoff and O'Shea, 2005; Hannich et al., 2005; Denison et al., 2005), with only a low level of overlap among studies in the sumoylated substrates that have been identified. Therefore, it is likely that there are many more transiently sumoylated substrates in yeast that have not yet been identified. These transiently sumoylated substrates might not be present in sufficient quantities in a steady-state cell population to be detected by normal methods; it is likely that they can only be detected using targeted methods, such as enriching cell populations in specific cell cycle stages and performing sensitive mass spectrometric analysis on proteins recovered from these enriched cell populations.

The goal of my dissertation research was to gain a greater understanding of the anaphase stage of mitosis through an investigation the proteins that localize to the spindle midzone, the region of microtubule overlap during anaphase spindle elongation. I focused on an investigation of the characteristics and interactions of two microtubule-associated proteins, Stu1 (CLASP homolog) and Slk19 (CENP-F homolog). Because Stu1 is essential for viability, I first investigated its characteristics and protein interactions to identify its essential function at the spindle midzone. I identified a number of physical interactors of Stu1 through mass spectrometric and yeast two-hybrid analyses and a number of genetic

interactors through a genetic synthetic lethality analysis. I also assessed the localization of Stu1 protein in live cells under a variety of mutant conditions (*slk19Δ* and *ase1Δ* cells) and obtained a better understanding of the Stu1 protein itself through mutation and truncation analyses and purification of the full-length protein. Through these investigations, I expanded the protein interaction network surrounding Stu1 and identified a number of interesting interactions and interdependencies among mitotic proteins. In particular, I identified a physical interaction between Stu1 and the mitotic protein Slk19, which also localizes to the kinetochores and spindle midzone during mitosis and plays an important role in anaphase progression through the regulation of Cdc14 phosphatase function.

Through my subsequent investigation of Slk19 function, I have identified a novel role for this protein in the regulation of Cdc14 at the end of anaphase. I determined that Slk19 is sumoylated in vivo and determined that a defect in sumoylation of Slk19 affects Cdc14 localization at the end of anaphase, just prior to mitotic exit. I then analyzed the effects of this change in Cdc14 localization on mitotic exit and found that premature movement of Cdc14 from the nucleus to the bud neck leads to rescue of a mitotic exit defect. Based on this research, I have provided a better understanding of the regulation of anaphase progression and mitotic exit as mediated by sumoylation of the FEAR network protein Slk19.

Chapter 2: Genetic, cell biological and biochemical characterization of the microtubule-associated protein Stu1 and its potential roles in mitotic progression

2.1 Introduction

Microtubule-associated proteins (MAPs) perform many important functions in mitosis. Some of the most important functions are the maintenance of the mitotic spindle to allow proper chromosome segregation. CLASP (Cytoplasmic Linker ASsociated Protein), which represents a family of homologous proteins conserved in all eukaryotes, is one class of MAP that is involved in spindle maintenance. CLASPs have a number of protein-protein and microtubule-binding interactions, and some CLASPs have been characterized as directly affecting microtubule dynamics (Maiato et al., 2005; Hannak and Heald, 2006; Al-Bassam et al., 2010). While all CLASPs share sufficient amino acid sequence homology to be included in the CLASP family, many specific protein-protein interactions and microtubule-binding domain sequences are unique to particular family members, indicating a range of functions among CLASPs from various eukaryotes.

The first CLASP discovered was *S. cerevisiae* Stu1 (Pasqualone and Huffaker, 1994). In 2000, two independent groups discovered Drosophila MAST/Orbit, and a CLASP family was recognized. These groups showed that MAST/Orbit is a microtubule-associated protein and is essential for mitosis in Drosophila (Inoue et al., 2000; Lemos et al., 2000). Since 2000, CLASPs have been identified in many eukaryotes, including numerous species of fungi, plants and animals (reviewed in Galjart, 2005). The CLASP family is so named because mammalian CLASPs interact with the CLIP (Cytoplasmic LInker Protein) family of MAPs (Akhmanova et al., 2001), which were characterized as microtubule-binding proteins that mediate interactions between organelles and microtubules (reviewed in Galjart, 2005).

CLASPs generally localize to both nuclear and cytoplasmic microtubules and are often concentrated at microtubule plus ends due to preferential plus end binding affinity (Mimori-Kiyosue et al., 2005; Reis et al., 2009). CLASPs generally share several physical characteristics, including a serine/arginine-rich region, numerous HEAT repeats (Huntingtin, Elongation factor 3, PR65/A subunit of protein phosphatase A, TOR; made up of two antiparallel α-helices), a CLIP-binding domain, an EB1 -binding domain and a microtubule-binding domain (reviewed in Galjart, 2005). EB1 (End-binding protein 1) is a microtubule-associated protein; EB1 interacts with Adenomatous Polyposis Coli (APC) protein (Su et al., 1995). Stu1, the *S. cerevisiae* CLASP, has a serine/arginine-rich region, HEAT repeats and a microtubule-binding domain, but it lacks a CLIP-binding domain and EB1-binding domain. Mammalian CLASPs have an additional domain at their N-termini, a TOG domain (Tumor Over-expressed Gene; made up of a number of HEAT repeats) (Charrasse et al., 1998; Al-Bassam et al., 2010); variants of this domain, termed TOG-like domains, also appear to be present in Stu1 (S. Harrison, Harvard University, personal communication). Other proteins with Dis1/TOG domains, namely the XMAP215 family of proteins, also play important roles in microtubule dynamics, so this domain may be important for microtubule interactions (Slep, 2009). Despite the fact that CLASPs have their own microtubule-binding regions, their interaction with EB1 seems to be important for proper microtubule binding and localization of metazoan CLASPs (Mimori-Kiyosue et

al., 2005). By contrast, Stu1 does not have a CLIP-170- or EB1-binding domain and has not been shown to interact with either CLIP-170 (Bik1) or EB1 (Bim1) in vitro or in vivo. Based on this evidence, it is likely that Stu1 can bind and properly localize to microtubules independently of Bik1 and Bim1.

The major investigated roles of CLASPs in mitosis are to regulate microtubule dynamics and stability. They have been shown to promote tubulin subunit addition at microtubule plus ends, which may be important for rescue of microtubule catastrophe (Maiato et al., 2004; Al Bassam et al., 2010). CLASPs have also been shown to stabilize overlapping arrays of mitotic spindles during mitosis without specific evidence of tubulin subunit addition; this stabilization may be related to its ability to add tubulin subunits to microtubule plus ends and is critical for mitotic progression and viability in yeast (Yin et al., 2002; Bratman and Chang, 2007). The S. cerevisiae CLASP, Stu1, plays an important role in spindle stability (Yin et al. 2002), but the mechanism of action of Stu1 on microtubule dynamics and stability is unknown.

In addition to influencing microtubule dynamics and stability in mitosis, some CLASPs affect microtubule dynamics during the interphase stage of the cell cycle. *S. pombe* CLASP stabilizes overlapping microtubule arrays (Bratman and Chang, 2007) and regulates mitochondrial distribution (Chiron et al., 2008) in interphase cells. In mammalian cells, CLASPs regulate microtubule plus end dynamics in the cytoplasm at the cell cortex (Lansbergen et al., 2006). By contrast, Stu1 has never been observed outside the nucleus in (Yin et al., 2002; personal data). Based on these data, and in contrast to metazoan and *S. pombe* CLASPs, Stu1 may only affect microtubule dynamics in the nucleus during mitosis.

STU1, which stands for Suppressor of tubulin mutation, was first identified as a gene that, when mutated, suppresses a cold-sensitive β-tubulin mutation (Pasqualone and Huffaker, 1994). The first isolated *stu1* mutations were not viable at 37ºC, and deleting the gene caused lethality after one or two cell divisions. Stu1 binds directly to microtubules, and *stu1* truncation mutants were used to identify a putative microtubule-binding region (Pasqualone and Huffaker, 1994). Stu1 was later shown to bind β-tubulin directly, and *STU1* loss-of-function mutations lead to mitotic spindle collapse and cell cycle arrest at metaphase (Yin et al., 2002). This phenotype correlates well with the cellular localization pattern of Stu1, as it associates with kinetochores, the pre-anaphase short mitotic spindle and the anaphase spindle midzone (Yin et al., 2002). These results indicate that Stu1 is involved in mitotic microtubule stability but do not reveal the mechanism of its involvement.

One feature of Stu1 that has made it difficult to dissect Stu1 molecular function in mitosis is its lack of recognizable protein domains. While Stu1p has an empirically determined microtubule-binding domain (Pasqualone and Huffaker, 1994), the region is not homologous to the microtubule-binding domains of other CLASPs (my data), and Stu1 does not associate with either EB1 or CLIP-170 by yeast 2-hybrid or mass spectrometric analysis (Wong et al., 2007; my data). Bioinformatics analyses have suggested the presence of a Dis1/TOG-like domain in Stu1 (S. Harrison, Harvard University, personal communication). A search of the PFAM (Protein FAMily) database (http://pfam.sanger.ac.uk/) revealed, however, that much of the Stu1 sequence consists of an armadillo-like repeat domain. Armadillo-like repeat sequences are related to HEAT repeats in that they are both composed of α-helices (reviewed in Andrade et al., 2001), and

both types of repeats are associated with protein-protein interactions. Based on this information, it seems likely that Stu1 contributes to spindle stability and mitotic progression through interactions with other proteins in addition to binding to tubulin proteins. However, Stu1 protein-protein interactions have not been studied in detail, and large-scale interaction studies have revealed few mitotically active Stu1p-interacting proteins. Because of this lack of information, it has been difficult to identify protein-protein interactions that help to inform the molecular function of Stu1 in mitosis.

Although data to support Stu1 protein-protein interactions are lacking, a group has recently shown that Stu1 may associate with centromeric DNA (Ma et al., 2007). Chromatin immunoprecipitation (ChIP) experiments using yeast centromeric DNA sequences demonstrated an interaction between Stu1 and CEN DNA *in vivo*. This result makes sense given that Stu1 localizes in the vicinity of kinetochores, which are closely associated with CEN sequences, during metaphase (Yin et al., 2002). However, these data do not provide evidence for Stu1p's mechanism of action because ChIP experiments cannot distinguish between direct and indirect DNA-protein interactions and do not imply any potential activity of Stu1p. A recent study, however, has provided insight into the possible function of Stu1 at kinetochores. This study found that Stu1 is preferentially localized to unattached kinetochores and only localizes to the spindle midzone upon proper kinetochore-microtubule attachment and relief of the spindle checkpoint (Ortiz et al., 2009).

The biochemical activities of Stu1's closest homologs have not been studied *in vitro*. However, a distant homolog of Stu1, *S. pombe* CLASP, has been studied in some detail. S. pombe CLASP helps to stabilize microtubule arrays, both in interphase and in mitosis, and promotes tubulin subunit addition at the microtubule plus end (Bratman et al., 2008; Al-Bassam et al., 2010). Therefore, *S. pombe* CLASP data confirm initial theories about the role of CLASPs in microtubule stability and might provide clues regarding the mechanism of action of Stu1.

This chapter presents the results of my varied scientific approaches to address the question of the mechanism of action of the *S. cerevisiae* CLASP, Stu1. Because Stu1 is one of the few essential spindle midzone proteins, I sought to understand its essential function and its role in spindle dynamics in anaphase. I investigated the role played by Stu1 in mitosis through genetic and physical interaction studies, phosphorylation studies, live cell microscopy of fluorescently tagged Stu1, and biochemical analyses of purified Stu1 protein. I collaborated with Professor John Yates at Scripps Research Institute in mass spectrometric studies and confirmed that Stu1 is highly phosphorylated in asynchronous culture, indicating a high level of steady-state phosphorylation. Stu1 is phosphorylated on a Cdk1 consensus site but found that mutation of this site does not affect mitotic progression or mitotic spindle dynamics. Through mass spectrometric analysis, I also identified a Stu1-interacting partner, Slk19, which is a protein that also localizes to the spindle midzone during anaphase and has known roles in mitosis, as well as a number of probable interacting partners. A yeast 2-hybrid analysis, which I carried out in collaboration with Professor Stan Fields' group at the University of Washington, revealed a number of direct or indirect interacting partners of Stu1, including two components of the sumoylation pathway. I carried out synthetic genetic analyses that showed that *stu1-5* is synthetic lethal with a number of genes that code for proteins involved in mitosis. I generated a number of C-terminal truncations of the Stu1 protein that found that they mislocalize within the nucleus during mitosis, indicating a requirement for specific regions of the protein for

proper midzone localization. Finally, my attempts to purify Stu1 protein from insect cells revealed that Stu1 protein is prone to degradation and aggregation. I also found, based on the point of elution of Stu1 from a gel filtration column, that Stu1 might have an elongated form, causing it to pass through the column at a higher apparent molecular weight than its actual molecular weight (Erikson, 2009), which is consistent with its high α-helical content.

2.2 Results

Stu1 interacts with a number of proteins in vivo by yeast 2-hybrid

To understand the mechanism of the activity of Stu1 and its role in mitosis, I identified a number of proteins that interact with Stu1 in vivo by yeast 2-hybrid (Y2H; James et al., 1996) in collaboration with Professor Stan Fields' group at the University of Washington. A previous study, carried out in my lab, identified two Stu1-interacting partners by Y2H, Bub1 and Trz1 (Wong et al., 2007); Bub1 plays an important role in the spindle checkpoint (Roberts et al., 1994), but Trz1, which is tRNAse Z, is a ribonuclease with no known role in mitosis (Chen et al., 2005). I cloned Stu1 Y2H baits of varying lengths (aa 1-500, 501-1,000 and 1,001-1,513) and full-length Stu1 baits with two different amino acid linkers (AAAAA and GGSGGSG) between the Stu1 N-terminus and the Gal4 DNA-binding domain to facilitate Y2H interactions (Figure 1). The aim was to identify novel Stu1-interacting partners and to determine whether different regions of the Stu1 protein have specific interacting partners. In this way, it would be possible to identify specific functional domains in Stu1, which had not been possible through bioinformatics approaches.

The interacting partners of the Stu1 bait proteins are listed in Table 1. Of these proteins, there were only two interacting partners that are relevant to mitosis, Nfi1 and Ubc9. Ubc9 (SUMO-conjugating enzyme) and Nfi1 (SUMO ligase) are interesting interactors because of the growing interest in the roles of sumoylation in mitosis (reviewed by Dasso, 2008). This finding suggests that Stu1 might be sumoylated in vivo; however, Stu1 has not been identified in any of the large-scale yeast sumoylation screens to date. Another possibility is that Ubc9 and Nfi1 interact with Stu1 indirectly, through their interactions with another Stu1-interacting protein, Slk19 (discussed below and in Chapter 3). As will be discussed further in my studies of Slk19, presented in Chapter 3, Slk19 interacts with Ubc9 by Y2H (Wong et al., 2007) and is sumoylated in vivo (my personal data).

Other than Ubc9 and Nfi1, there were no interacting preys that seem to give insights into the mitotic function of Stu1. Unexpectedly, Slk19, which interacts with Stu1 by mass spectrometry (discussed below), was not identified as an interacting prey, which validated my decision to identify physically interacting proteins by another method, mass spectrometry, in addition to the Y2H approach. Moreover, the only prey that interacted with two Stu1 baits was BDF2, whose protein product Bdf2 is involved in transcription initiation at TATA-binding promoters (Matangkasombut et al., 2000). In fact, the largest single group of interacting preys are DNA-interacting proteins (25%; 15 out of 60 preys identified). This finding suggests that Stu1 might directly interact with DNA, in agreement with recent studies that found that Stu1 interacts with centromeric DNA (Ma et al., 2007)

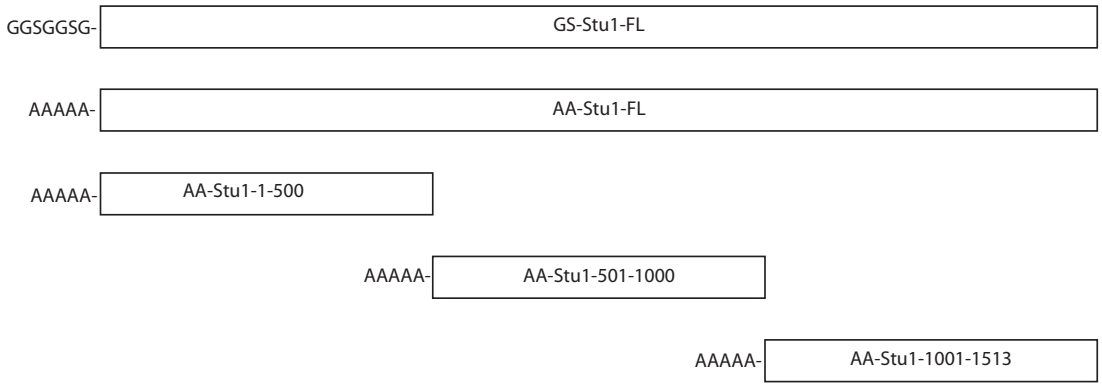

Figure 1. Schematic of Stu1 bait constructs for yeast two-hybrid assay. N-terminal flexible amino acid sequences are shown to the left of each construct; full-length and truncation constructs are shown approximately to scale with respect to the truncation points.

Table 1. Results of yeast two-hybrid analysis of full-length and fragmented *STU1* baits

	Bait that pulled down each prey				
Prey name	GS-Stu1-FL	AA-Stu1-FL	AA-Stu1-1-500	AA-Stu1-501-1000	AA-Stu1-1001-1513
ACF4			+		
AFG2	+				
AIM1	+				
ART10			+		
BDF2	+		+		
CAC2		+			
EFT1			+		
ECM15			+		
FLO10			+		
FUI1			+		
GIS4			+		
GTT3	+				
HAP2			+		
HHF2			+		
HPC2	+				
KAE1	+				
KTR4	+				
MCH2			+		
MIG2			+		
MRPS18	+				
MXR1	+				
NAM7					+
NBP2					+
NFI1	+				
PHR1	+				
PKH3	+				
PRP18	+				
PSY4	+				
RAD27			+		
RAD34	+				
RCR2	+				
REV7	+				
RMI1	+				
RPL22A	+				
RRG8			+		
SGS1	+				
SHR3	+				
SNG1	+				
SPB1			+		
STE11	+				
STN1	+				
SUP45	+				
TAF10	+				
TEF4	+				
TOD6	+				
UBC9					+
ULA1	+				
URN1	+				

VHS3		+		
YAR068W	+			
YBL095W	+			
YBR047W				+
YCR101C				+
YFH1	+			
YFL051C	+			
YGR125W	+			
YHR177W				+
YJL113W				+
YMR130W				+
YRF1-6	+			

Prey constructs that interacted with Stu1 bait constructs by yeast 2-hybrid. "+" indicates an interaction. The labels "GS" and "AA" indicate the flexible amino acid linker sequences GGSGGSG and AAAAA, respectively. The prey BDF2 is highlighted because it was found to interact with both GS-Stu1-FL and AA-Stu1-1-500. The preys designated "YXXXXXW/C" represent uncharacterized open reading frames (ORFs).

and that Stu1 preferentially associates with unattached kinetochores during metaphase (Ortiz et al., 2009). However, the activity of Stu1 at DNA remains unknown.

With regard to the Y2H assay itself, the fact that there was no overlap in the results obtained between full-length Stu1 bait constructs that differed only in the length of the flexible amino acid linker attached between Stu1 and the Gal4 DNA-binding domain indicates that one or both of these full-length baits was not fully functional or may have undergone intracellular degradation. This lack of overlapping interaction data may also be indicative of the Gal4 DNA-binding domain being cleaved off of the Stu1 bait. This possibility is made more likely by the result that a number of known false positive preys (*MIG1*, *MIG3*, *GAL4*, *TID3*; S. Nelson, University of Washington, personal communication) were identified as interacting with various Stu1 baits (data not shown). With optimization of the Stu1 bait construct with respect to the location of the Gal4 DNA-binding domain and the choice of flexible amino acid linker sequence, additional Y2H interacting preys might be identified.

Stu1p interacts with Slk19p in vivo

As a second approach to identify proteins that interact with Stu1 in vivo, I purified from yeast Stu1 protein that was fused to a C-terminal tandem affinity purification (TAP) tag (Cheeseman et al., 2001) and, in collaboration with Professor John Yates' group at Scripps Research Institute, identified the proteins that interacted with Stu1 *in vivo*. The initial list of interacting proteins is listed in Table 2. There were relatively few proteins that interacted with Stu1 under the purification conditions used (150 mM NaCl, which is a relatively low-salt condition), but one interacting protein identified was Slk19p. I was very interested in obtaining Slk19 as a protein interacting with Stu1 because Slk19 also localizes to the spindle midzone during anaphase (Zeng et al., 1999). After obtaining this interaction result, I attempted to determine if the Stu1/Slk19 interaction was robust enough to be detected in a co-immunoprecipitation (co-IP) experiment. However, I was unable to immunoprecipitate Stu1. This inability to immunoprecipitate Stu1 may be due to its low abundance in the cell (approximately 521 molecules per cell; Ghaemmaghami et al., 2003) and/or the cell's tendency to delete C-terminal tags on Stu1 through some type of proteolytic cleavage (Figure 2). Due to the low abundance of Stu1 or some other unknown factor, Stu1 could also not be immunoprecipitated using an N-terminal GFP tag (data not shown). Therefore, there may be additional protein interacting partners of Stu1, but a different tagging and purification protocol will be necessary to identify them.

Stu1 is phosphorylated in vivo, but mutation of its Cdk1 consensus site does not affect spindle dynamics or organization

As part of the mass spectrometric analysis of Stu1 and because many MAPs have phosphorylation-dependent functions, the Yates lab performed a phospho-enrichment and phosphopeptide analysis of the Stu1-TAP protein sample. We found that Stu1 is highly phosphorylated; 23 serine or threonine phosphorylation sites were identified with 92% or better confidence; no phosphorylated tyrosines were detected (Table 3). These sites were distributed throughout the Stu1 protein sequence and seemed to have a slight bias toward

Table 2. Results of mass spectrometry of Stu1-TAP purification

Protein name	# of peptides detected	Expected # of peptides	Enrichment
Stu1	1218	2	60,900%
Slk19	94	25	375%
Ssa2	35	39,187	none
Ssb1/Ssb2	7	32,194	none
Bmh1/Bmh2	7	6,176	none

All proteins that were detected in a Stu1-TAP purification by MALDI-TOF mass spectrometry. Protein sequence coverage was compared to expected sequence coverage based on Peptide Atlas results for non-enriched yeast mass spectrometry analyses of wild type yeast (peptideatlas.org). Proteins with sequence coverage below expected coverage for wild type cell analyses were considered not enriched ("none").

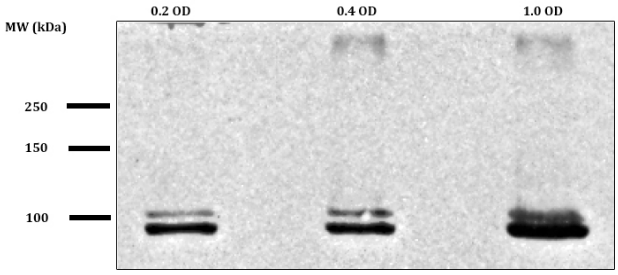

Figure 2. C-terminal 3xGFP tag is cleaved off of Stu1-3xGFP. Western blot probed with α-GFP antibody. Lanes represent increasing numbers of cells (in OD_{600} equivalents) loaded on gel. Expected size of 3xGFP is approximately 90 kDa. Expected size of Stu1-3xGFP is approximately 265 kDa.

Table 3. Results of Stu1-TAP phosphoenrichment mass spectrometry

Protein name	Sequence coverage (%)	Number of phosphoresidues	Identities of phosphoresidues
Slk19	39	2	S216, S279
Stu1	35	22	T496, S497, S619, S621, T622, S634, S669, T719, S741, S793, S1001, T1005, T1034, T1047, S1077, T1080, S1105, S1108, S1113, S1119, T1165, S1167, T1193
Igo1	21	1	T140
Ssa1	16	1	T549
Tif34	6	2	S302, S307
Mak32	5	2	T274, S287
Bet4	5	2	Y26, Y28
Otu1	4	1	Y213
Nba1	4	3	T384, S385, T386
Doa4	2	1	S49
Red1	2	2	S243, T245
Ctk1	2	1	S430
Sro77	2	1	T717
YDL109C	2	1	Y63
Rot2	1.5	2	S818, Y827
Tif4631	1.5	1	Y75
Sap185	1	1	S81
Bni1	<1	1	S1820
Tra1	<1	1	Y2550
Ssa2	15	-	
Rps3	7	-	
Bmh1/Bmh2	7	-	
Erg29	6	-	
YGR126W	6	-	
YPR127W	4	-	
Ssc2	4	-	
Gpa2	4	-	
Nop13	3	-	
Snu56	3	-	
Smp2	1.5	-	
Tcb1	1	-	
Smc1	1	-	
YPR117W	<1	-	

All proteins that were detected after enriching for phosphopeptides in a Stu1-TAP purification using a TiO_2 column. A number of proteins were detected in this phosphopeptide enrichment analysis but were not detected as phosphorylated by mass spectrometry (proteins below the solid line).

the C-terminus; however, the sequence coverage of the N-terminus (including the microtubule-binding region) was low, so additional sites may be present in this region (Figure 3A). The identification of phosphorylated Stu1 is in agreement with my experimental results that Stu1 protein undergoes a clear band shift when treated with alkaline phosphatase to remove all phosphorylation events (Figure 3B).

While few of these phosphorylated residues matched known kinase consensus sites, one site, S1167 (S*PIK), matched the strict Cdk1 consensus site [ST][P][X][KR]. Therefore, I mutated this residue to alanine (A; phosphomutant) or aspartic acid (D; phosphomimic) to investigate the biological significance of this phosphorylation by evaluating the phenotypes of the mutant proteins. I integrated the two point mutants into the native *STU1* locus to assess these mutant proteins at endogenous levels. The mutants had no growth defect compared to wild type Stu1, and spindle dynamics were not affected by either mutant ($p > 0.2$ for all pairwise comparisons; Figures 4A-D). Moreover, the localization pattern of the spindle midzone marker Ase1 was not affected by either mutant (Figure 5). Therefore, I concluded that mutation of the Cdk1 consensus site of Stu1 to alanine or aspartic acid did not affect its function in spindle stability or mitotic progression.

In addition to Cdk1, there are a number of other mitotically active kinases, including Aurora B kinase, Polo-like kinase, casein kinase 2, the spindle checkpoint kinases Bub1 and Mps1 and the MEN kinases Dbf2 and Cdc15. Unfortunately, there were no phosphorylated residues that matched the consensus sequences for casein kinase 2, Aurora B kinase or Polo-like kinase. The other mitotic kinases have no known consensus sequences. This difficulty in predicting which kinase or kinases are responsible for the various phosphorylation events of the Stu1 protein highlights the general difficulty in predicting kinase targets. Most kinases have only a loose consensus sequence, if one exists at all. In addition, many "non-consensus" phosphorylation events have been detected *in vitro* and *in vivo*. Therefore, a combined genetic and biochemical approach of using analog-sensitive alleles of various mitotic kinases coupled with the detection of a band shift of phosphorylated Stu1 protein might provide new information regarding the kinase(s) responsible for these phosphorylation events.

STU1 interacts with a number of genes coding for proteins involved in mitosis

In our laboratory and others, genetic synthetic lethality analysis has been used to place genes and their corresponding proteins in discrete pathways to better understand their mechanisms of action. To analyze the role of Stu1 in mitotic progression, I performed a small-scale synthetic lethality screen between *stu1-5* (temperature-sensitive allele of *STU1* (Pasqualone and Huffaker, 1994)) and a number of genes encoding proteins involved in mitosis. Prior to my study of Stu1, *stu1-5* was previously shown to be synthetic lethal with several mitotic proteins: Bim1 and Dam1, which are MAPs; Yke2, Pac10, Gim3, Gim4 and Gim5, which are components of the prefoldin chaperone complex that aids in the folding of cytoskeletal proteins (reviewed in Lopez-Fanarraga et al., 2001); Kem1, an exonuclease involved in mRNA decay (Solinger et al., 1999), and Ubp3, a ubiquitin-specific protease (Baker et al., 1992). However, there were a number of other candidate genes with roles in mitosis that had not been assessed for genetic interactions with *stu1-5*. The full list of synthetic interactions that I obtained is shown in Table 4A. The strongest synthetic

A

```
1    MSSFNNETNN NSNTNTHPDD SFPLYTVFKD ESVPIEEKMA LLTRFKGHVK
51   KELVNESSIQ AYFAALLFIS GHYAYRSYPR LIFLSHSSLC YLIKRVAMQS
101  PVQFNDTLVE QLLNHLIFEL PNEKKFWLAS IKAIEAIYLV NPSKIQAILA
151  NFLRRPSENQ NGDYLNRIKS TLLTIDELIQ INEKNNSNHL QLLRFFMLSF
201  TNLLNNNLNE HANDDNNNVI IELIFDIMYK YLKMDDENSQ DLIDGFINDL
251  EVEKFKQKFI SLAKSQDQHG SQEDKSTLFD EEYEFQLLLA EAKLPQLSNN
301  LSSKDPAMKK NYESLNQLQQ DLENLLAPFQ SVKETEQNWK LRQSNIIELD
351  NIISGNIPKD NPEEFVTVIK EVQLIELISR ATSSLRTTLS LTALLFLKRL
401  IHILNDQLPL SILDQIFVIF KNLLSSTKKI SSQTAFHCLI TLIIDINHFH
451  NKLFQLSFLL INEKTVTPRF CSAILLRSFL IKFNDSNLSL NNSNTTSPTS
501  KLENNIIYIE EWLKKGISDS QTTVREAMRL TFWYFYKCYP TNAKRLLSSS
551  FSPQLKKATE LAIPAHLNIN YQVSRVSSTA SASSATSRLY SHSSNNSSRK
601  TSLLEQKRNY PSYAQPTQSS STSLLNAPAV TAGGSVIASK LSNKLKTNLR
651  STSEYSSKEN EKRARHHDSM NSVSNSNTKD NNNVTKRKVS APPSSTAATK
701  VSENYTNFDD FPSNQIDLTD ELSNSYSNPL IKKYMDKNDV SMSSSPISLK
751  GSNKLGEYET LYKKFNDASF PAQIKDALQY LQKELLLTSQ QSSSAPKFEF
801  PMIMKKLRQI MIKSPNDFKP FLSIEKFTNG VPLNYLIELY SINSFDYAEI
851  LKNRMNPEKP YELTNLIITI ADLFNFLNAN NCPNDFKLYY MKYKTTFFNY
901  NFKLLLEIFR NLNIKHDNTL RSGTNDLMPK ISMILFQIYG KEFDYTCYFN
951  LIFEIYKFDN NRFNKLLADF DIVSTKMKIC HELEKKDANF KVEDIISRES
1001 SVSFTPIDNK KSEGDEESDD AVDENDVKKC MEMTMINPFK NLETDKTLEL
1051 KNNVGKRTSS TDSVVIHDDN DKDKKLSEMT KIVSVYQLDQ PNPAKEEDDI
1101 DMENSQKSDL NLSEIFQNSG ENTERKLKDD NEPTVKFSTD PPKIINEPEK
1151 LIGNGNENEK PDLETMSPIK INGDENMGQK QRITVKRERD VALTEQDINS
1201 KKMKLVNNKK SEKMHLLIMD NFPRDSLTVY EISHLLMVDS NGNTLMDFDV
1251 YFNHMSKAIN RIKSGSFTMK HINYLIEPLI TCFQNQKMTD WLTNENGFDE
1301 LLDVAIMLLK STDDTPSIPS KISSKSIILV HCLLVWKKFL NTLSENADDD
1351 GVSVRMCFEE VWEQILLMLN KFSDYGNEIY KLAQEFRDSL MLSHFFKKHS
1401 ATRILSMLVT EIQPDTAGVK ETFLIETLWK MLQSPTICQQ FKKSNISEII
1451 QTMSYFIMGT DNTSWNFTSA VVLARCLRVL QTTPDYTEQE TERLFDCLPK
1501 NVFKMIMFIA SNE*
```

B

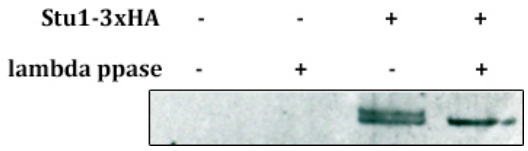

Figure 3. Stu1 is a phosphoprotein. (A) Mass spectrometry results of purified Stu1 expressed in yeast. Blue residues represent sequences detected in mass spectrometry analysis; gray residues represent sequence that was not detected; red residues represent phosphorylated residues. (B) Western blot of the phosphoprotein Stu1-3xHA incubated in the presence or absence of lambda phosphatase. Stu1-3xHA was immunoprecipitated from yeast using a-HA antibody before being loaded onto the gel. In the presence of lambda phosphatase (far right lane), the phosphoprotein doublet collapses into a single band.

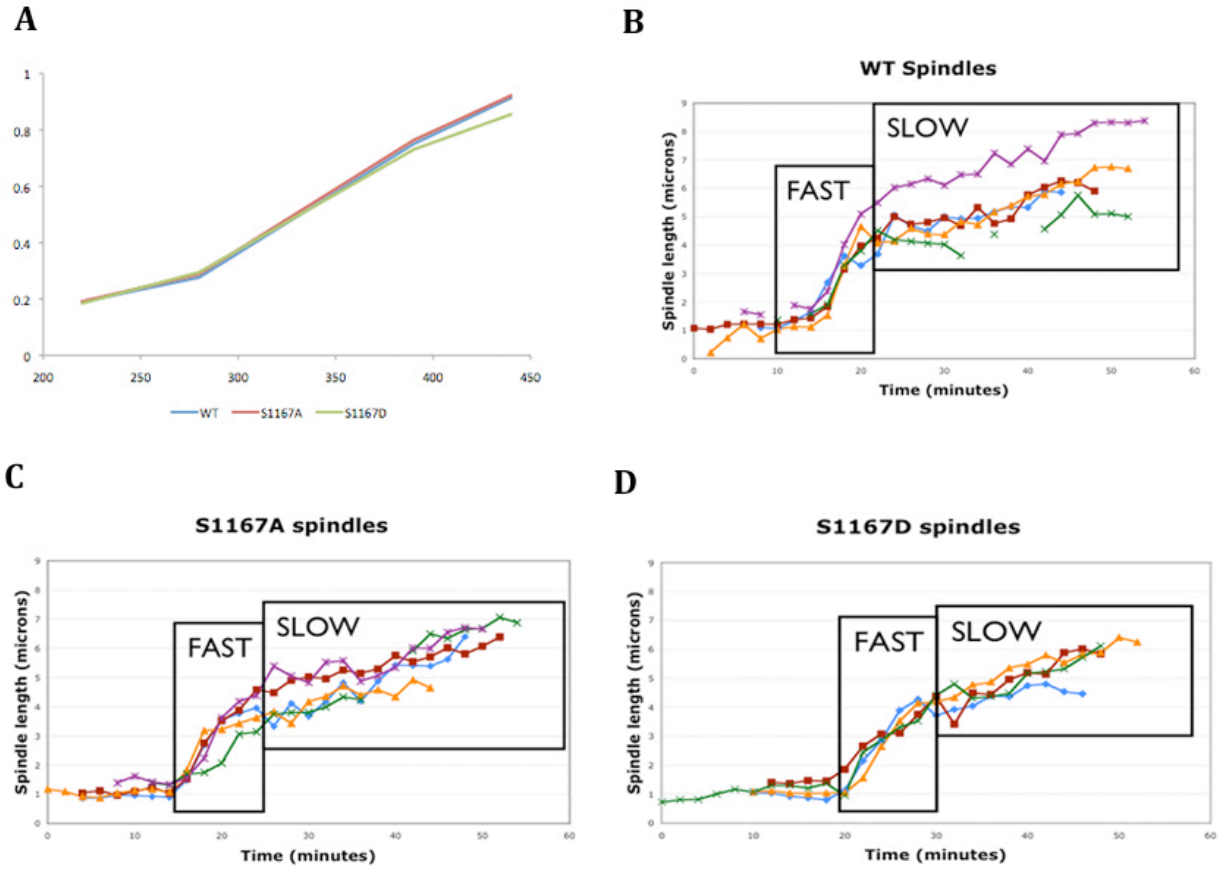

Figure 4. Mutation of the conserved Cdk1 site in Stu1 has no effect on cell growth or spindle dynamics in vivo. (A) log-phase growth curve of wild type Stu1 (blue) Stu1(S1167A) (red) and Stu1(S1167D) (green) in standard rich medium. (B-D) anaphase spindle traces of individual cells of each respective genotype. Each colored line represents an individual spindle. The fast and slow phases of spindle elongation are highlighted in boxes. The differences in the rates of the fast and slow phases between wild type Stu1, Stu1(S1167A) and Stu1(S1167D) are not significant.

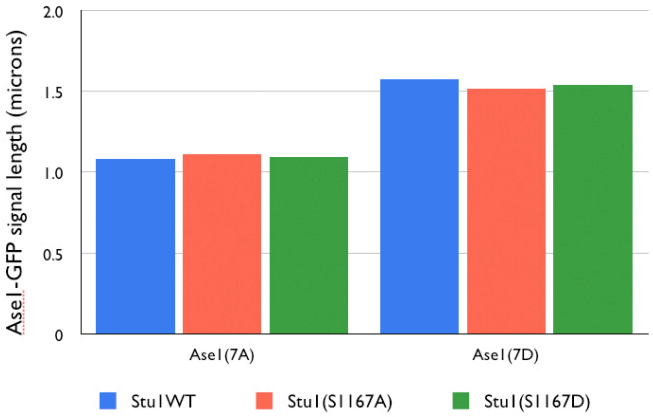

Figure 5. The width of the Ase1-GFP signal at the spindle midzone does not differ between wild type Stu1 and Stu1 phosphomutants. Ase1(7A)-GFP (all 7 Cdk1 sites mutated to alanine) and Ase1(7D)-GFP (all 7 Cdk1 sites mutated to aspartate) have significantly different signal spreads on the midzone, but these differences are not significantly modulated by wild type Stu1 (blue), Stu1(S1167A) (red) or Stu1(S1167D) (green).

Table 4A. Synthetic genetic interactions between *stu1* mutants and genes involved in mitosis

Gene name	Synthetic interaction?	Details of interaction
ASE1	Yes	50% decrease in viability
BUB1	Yes	Strong decrease in viability
MAD2	Yes	TS enhancement
IPL1	Yes	TS enhancement
DYN1	Yes	TS enhancement
BIM1	Yes	Strong decrease in viability
SLK19	No	N/A
KAR9	No	N/A
SKP1	No	N/A
MPS1	No	N/A
MAD3	No	N/A

Results of a synthetic genetic interaction analysis that I performed to identify additional genes that interact with *stu1-5*. Genes that, when combined with *stu1-5*, result in reduced viability even at the permissive temperature (25^{o}C) are designated "viability" effects. Genes that, when combined with *stu1-5*, result in reduced viability at a semi-restrictive temperature (30^{o}C) are designated "TS enhancement."

genetic interaction occurred between *stu1-5* and *bub1Δ*. As strong synthetic genetic interactions often indicate two proteins acting in parallel and/or complementary pathways, this finding might mean that Stu1 and Bub1 are acting in parallel pathways during mitosis. However, *stu1-5* was only synthetic lethal with some tested members of the spindle assembly checkpoint; it negatively interacted with *bub1Δ* and *mad2Δ*, but *mad3Δ* and *mps1-ts* had no negative interactions. These results imply that Stu1 acts in a pathway that might involve some, but not all, members of the known spindle assembly checkpoint. *stu1-5* was also synthetic lethal with some but not all tested MAPs. There were synthetic genetic interactions with *ase1Δ*, *bim1Δ*, *ipl1-ts* and *dyn1Δ* but not *slk19Δ* and *kar9Δ*. These results highlight the fact that there are parallel pathways at work for both spindle stability (involving Ase1, Slk19, Bim1 and Ipl1, among others) and spindle positioning (involving Dyn1 and Kar9, among others); based on the differential genetic interaction results, Stu1 is likely to be in the same pathway as Slk19 (due to the lack of genetic synthetic lethal interaction between *stu1-5* and *slk19Δ*) and might be involved in both spindle stability and spindle positioning. Using a number of unique temperature-sensitive *stu1* alleles, the Boone laboratory at the University of Toronto has confirmed the genetic interactions for *bim1Δ*, *dyn1Δ* and *mad2Δ* (Table 4B; personal communication). Subsequent large-scale studies by the Boone lab and others have confirmed most of the genetic interactions that I found in my study, including those between *stu1* and *ase1Δ*, *bim1Δ*, *dyn1Δ*, *bub1Δ* and *mad2Δ* (Amaro et al., 2008; Costanzo et al., 2010).

Stu1 C-terminal truncations have different localization patterns and differences in protein stability

Two of the difficulties that I encountered in studying Stu1 are its apparent lack of recognizable domains, based on protein sequence homology, and its low overall sequence homology to other members of the CLASP family. A recent PFAM (http://pfam.sanger.ac.uk/) domain analysis indicated that Stu1 possesses a "CLASP homology domain." In addition to this seemingly circular domain designation, Stu1 is believed to possess TOG-like domains in its N-terminus, overlapping with its microtubule-binding domain (S. Harrison, Harvard University, personal communication). Based on this scarcity of protein domain information, I assessed the cellular requirements of biological activity in spindle function of various regions of Stu1 using N- and C-terminal truncations and analysis of the resulting mutant proteins' phenotypes *in vivo*. The truncation points are shown in Figure 6A. The C-terminal truncations were all viable, but they resulted in aberrant protein localization patterns in live cells (Figure 6B); all Stu1 truncated proteins were localized to kinetochores prior to anaphase, but during anaphase, the truncated Stu1 proteins were either localized diffusely in the nucleus (in the case of Stu1(1-1453)) or had no detectable localization (in the cases of Stu1(1-750) and Stu1(1-750)), in contrast to wild type Stu1, which localized to the spindle midzone during anaphase. These findings indicate that the portion of Stu1 that is essential for overall cell viability is located in the N-terminal half of the protein and that the midzone localization pattern of Stu1 is not the primary effector of its essential function. It is possible that Stu1 C-terminal truncations still bind to microtubules at low levels; purification of these truncated proteins and in vitro microtubule binding experiments would be required to answer this question. Interestingly,

Table 4B. *stu1* synthetic lethal interactions at 30°C (courtesy of Boone Lab, U of Toronto)

Gene	*stu1-5*	*stu1-6*	*stu1-7*	*stu1-8*	*stu1-12*
BEM2			SL	SL	
BIM1	SL		SL	SL	
CLA4			SL	SL	
CTF4	SL	SL	SL	SL	SL
CTF8				SL	
DNM1			SL		
DOC1					SL
DRS2		SL		SL	
DYN1	SL			SL	
ELP2			SL		
GIM4	SL	SL			SL
HIT1			SL		
HLR1					SL
HXK2				SL	
KTR2		SL	SL		
MAD2	SL	SL		SL	SL
MCK1		SL			
MCM21	SL	SL		SL	SL
MED2			SL		
MRC1		SL			
MRT2		SL			
NUM1	SL	SL			SL
REI1			SL		
RFC5			SL		
RPN1				SL	
RPN10				SL	
RVS167			SL	SL	
SEC22				SL	
SET2				SL	
SHE1	SL	SL		SL	SL
SWR1		SL			
TIF3		SL			
TUB3	SL	SL		SL	SL
VPS35				SL	
YFL034W				SL	
YLR422W		SL			
YNL122C		SL		SL	
YOR072W-B	SL				SL
YPT6				SL	

All synthetic genetic interactions between various *stu1* temperature-sensitive alleles (*stu1-5-10*) and deletion mutants of the listed genes. This screen was performed at 30°C, a semi-restrictive temperature for *stu1* temperature-sensitive alleles. "SL" indicates a genetic synthetic lethal interaction. Highlighted genes represent genes that I also found to be synthetic lethal with *stu1-5*.

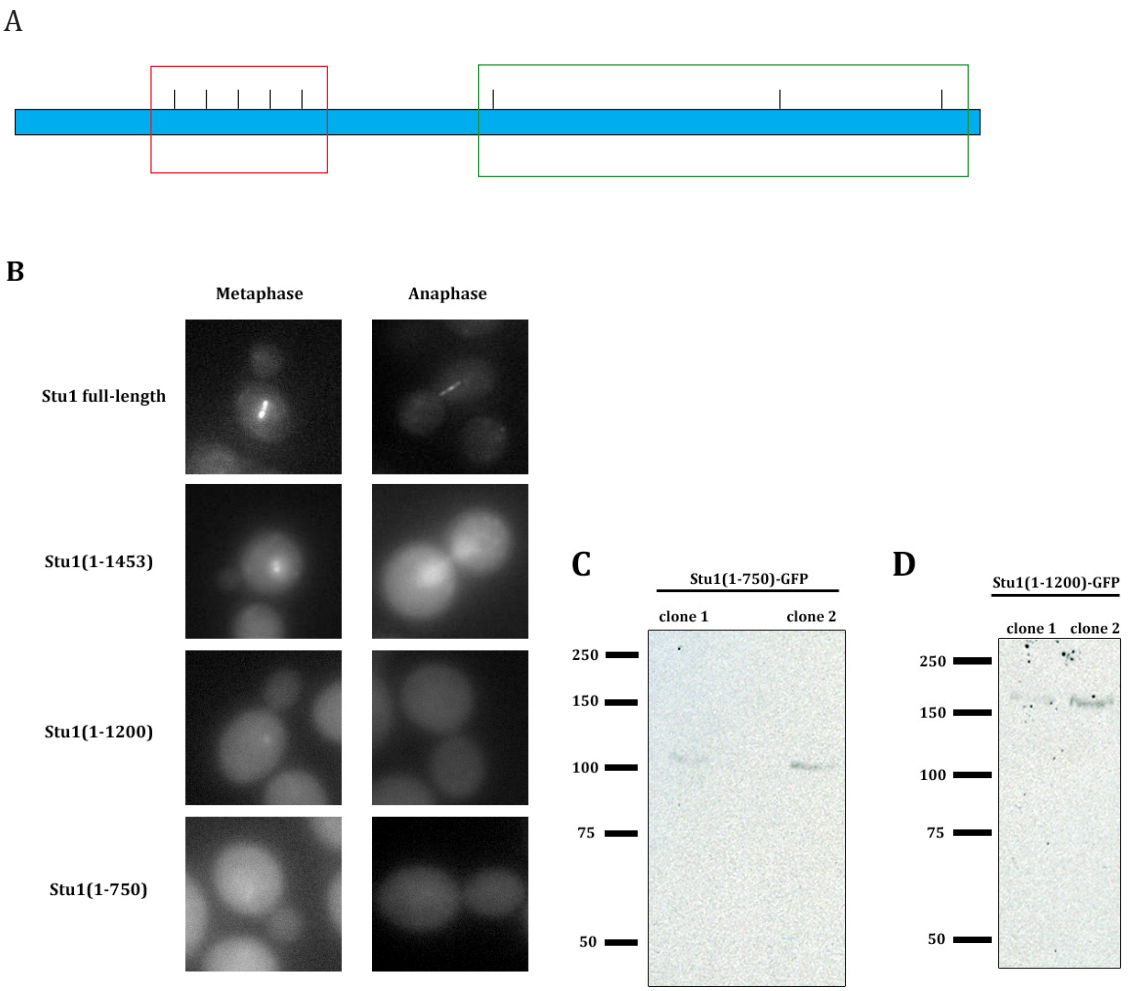

Figure 6. Stu1 C-terminal truncation mutants support viability but do not localize properly to spindles. (A) schematic of Stu1 protein and the locations of N- and C-terminal truncation points. N-terminal truncations (boxed in red), at 250, 300, 350, 400 and 450 amino acids, do not support viability. C-terminal truncations (boxed in green), at 750, 1200 and 1453 amino acids, support viability. (B) Live cell microscopy images of Stu1-GFP yeast strains during metaphase and anaphase. Images were taken at 100X magnification. (C and D) western blots, probed with α-GFP antibody, of Stu1(1-750)-GFP and Stu1(1-1200)-GFP isolated from cell extracts. Two clones for each truncation are shown for comparison. The expected sizes of Stu1(1-750)-GFP and Stu1(1-1200)-GFP are 117 kDa and 168 kDa, respectively.

while full-length, epitope-tagged Stu1 protein cannot be visualized in a whole cell extract by Western blot, the C-terminal truncations including aa 1-750 and 1-1200 can be detected under the same conditions (Figures 6C and D). Stu1(1-1453)-GFP could not be detected by western blot (data not shown). These findings indicate that when the C-terminus has been removed from Stu1 beyond the last 50 amino acids, there is no longer a tendency in the cell to cleave off a C-terminal tag. N-terminal truncations, however, including truncation of the first 250 amino acids of Stu1, were not viable, indicating that the essential function of Stu1 resides in the first 250 amino acids of the protein. This finding could indicate that the TOG-like domains, some of which are thought to reside in the first 250 amino acids of the protein, are an important part of the essential function of Stu1.

Stu1 protein purification

To achieve a better understanding of Stu1 activity, I sought to purify full-length Stu1 protein to perform in vitro microtubule dynamics assays and visualize Stu1 protein interacting with microtubules by electron microscopy. Attempts to purify Stu1 from yeast were not successful, resulting in extremely low protein yields (data not shown), so a baculovirus construct was made with an N-terminal 6xHis-tagged Stu1 protein. The tagged protein was expressed in SF9 insect cells. The protein was purified using an imidazole-based purification protocol (based on the QiaExpress system, Qiagen) and passage though a gel filtration column using fast protein liquid chromatography (FPLC). Representative protein gels from various steps of the purification procedure are shown in Figures 7A-C; the gel filtration trace from the FPLC is shown in Figure 7D. Based on the gel-filtration result, Stu1 appeared much larger than its predicted size of 174 kDa; its apparent size of 1.0 MDa indicates oligomerization or aggregation of purified Stu1 in solution. Another possibility is that Stu1 could be elongated in shape, which would cause it to run at an apparently higher molecular weight upon gel filtration than its true molecular weight (Erikson, 2009). If Stu1 formed a homotetramer and had an apparent molecular weight of approximately 250 kDa per monomer, the apparent molecular weight upon gel filtration would be approximately 1.0 MDa. Further co-sedimentation analysis of Stu1 to determine the protein's Stokes radius would be required to answer this question.

Stu1 mislocalization in *ase1Δ* and *slk19Δ* cells

To understand the interplay among different midzone proteins during anaphase, I first analyzed the localization pattern of Stu1-GFP in *ase1Δ* cells. Ase1 is considered the master scaffold protein at the spindle midzone during anaphase (Khmelinskii et al., 2007). In these cells, Stu1-GFP localized diffusely throughout the nucleus rather than specifically at the spindle midzone during anaphase (Figure 8A), suggesting that one of the functions of Ase1 is to allow the proper localization of Stu1 to the midzone. My finding was confirmed independently by Khmelinskii et al. (2007), who also found that Ase1 is required for the midzone localization of Stu1. Along with my Stu1 C-terminal truncation data, this finding suggests that the essential function of Stu1 does not depend on its spindle midzone localization, implying an as-yet-unidentified primary function of Stu1.

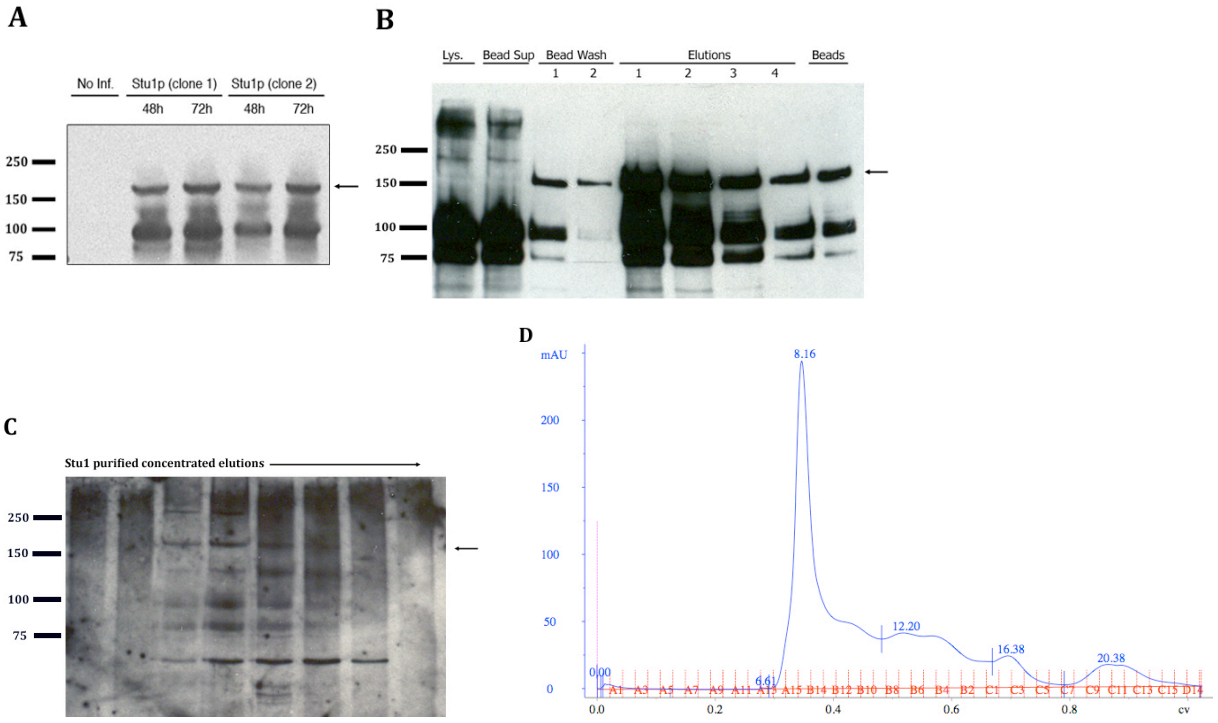

Figure 7. Stu1 purification from a baculovirus construct and SF9 insect cells. (A) Western blot, probed with α-His antibody, assessing the expression levels of baculovirus-expressed Stu1 clones from SF9 cell extracts. The expected size of 6xHis-Stu1 is approximately 175 kDa. Under standard conditions, a degradation product of approximately 95 kDa is routinely observed. (B) Western blot, probed with a-His antibody, of Stu1 purification from SF9 cells. Stu1, visible at approximately 160-175 kDa, is substantially purified from the cell lysate, but a number of degradation and/or contaminant bands are also present in the purified fractions (designated as "Elutions"). (C) Western blot, probed with a-His antibody, of concentrated fractions eluted from a gel filtration column to separate purified Stu1 and associated proteins by size. (D) FPLC trace of Stu1 eluted from a gel filtration column. The major fraction elutes at approximately 1.0 MDa, which is approximately 6 times larger than the expected size of the Stu1 monomer.

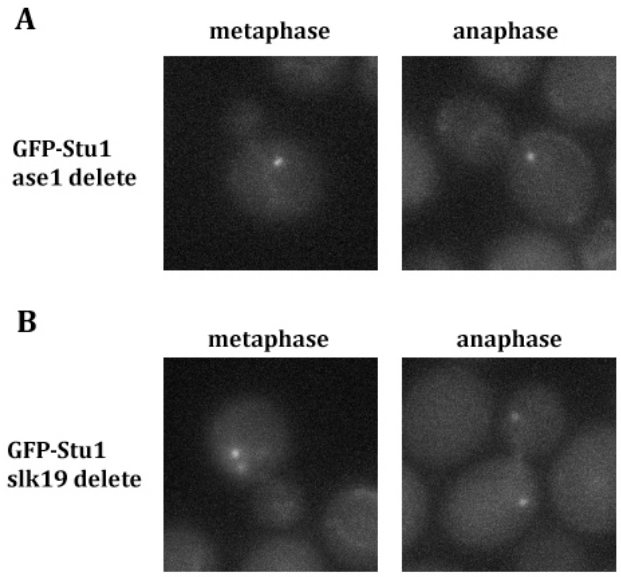

Figure 8. Mislocalization of Stu1 in cells lacking the spindle-associated proteins Ase1 and Slk19. Live cell microscopy images of GFP-Stu1 in (A) *ase1Δ* cells and (B) *slk19Δ* cells. Representative metaphase and anaphase cells are shown for each mutant condition. In *ase1Δ* cells, GFP-Stu1 localizes to the kinetochores in both metaphase and anaphase; in *slk19Δ* cells, GFP-Stu1 is localized to the kinetochores during metaphase and the kinetochores and spindle during anaphase, but the spindle localization is significantly decreased and kinetochore localization significantly increased compared to wild type (see Figure 6B).

I had previously demonstrated that Stu1 physically interacts with Slk19. Therefore, I wanted to understand whether Stu1 required Slk19 for its microtubule and/or midzone localization. In contrast to the effects seen by Khmelinskii et al., who observed continued localization of Stu1 to a spindle midzone that was shifted to either the mother or daughter cell in a *slk19Δ* background, I observed that in the absence of *SLK19*, Stu1 had a dramatically decreased spindle midzone localization (Figure 8B). In addition, Stu1 continued to localize to the kinetochores during anaphase, a localization pattern that is never observed for Stu1 in a *SLK19* wild type strain. These results indicate that Slk19 is involved in the relocalization of Stu1 from the kinetochores to the spindle midzone upon anaphase onset. The *slk19Δ* cells are viable, so full relocalization of Stu1 from the kinetochores to the spindle midzone is not essential, in agreement with data from my and other studies (Khmelinskii et al., 2007). However, the decreased ability of Stu1 to localize to the spindle midzone in *slk19Δ* cells could be an explanation for why these cells have fragile spindles and decreased spindle stability during anaphase.

2.3 Discussion

Since the identification of Stu1 in 1994, many studies have been performed on this family of proteins called CLASPs across the spectrum of eukaryotic organisms. These studies have shown that while CLASPs have a core subset of conserved functions and characteristics, they are a relatively heterogeneous family in terms of their roles in mitosis. Attempts to generalize and categorize all CLASPs as having certain characteristics (for example, the ability to bind the plus ends of microtubules) may be obscuring the heterogeneity of their functions as well as their essential mechanisms of action. In particular, the functions of fungal CLASPs seem to have diverged considerably from animal CLASPs. This divergence could be due to the differences in the organization of the microtubule-based spindle and kinetochore-microtubule attachments between fungi and animals.

Stu1, which is a CLASP by way of its limited amino acid sequence homology and ability to bind microtubules, does not necessarily act as a plus end tracking protein. It decorates the spindle midzone during anaphase, which could be a result of either its affinity for the plus ends of microtubules or its affinity for antiparallel microtubules. Its primary function in anaphase might be as a spindle midzone stabilizer, evolving from the budding yeast's need for strong stabilization at a particularly fragile midzone. Future studies that assess the interaction between purified Stu1 and microtubules in vitro, through bundling and microtubule dynamics assays, will be required to test this hypothesis.

The yeast two-hybrid results that I obtained using the Stu1 baits that I constructed were unexpected in that they did not demonstrate that Stu1 interacts with other microtubule-associated proteins. The fact that 25% of the identified preys were DNA-interacting proteins indicates that a major function of Stu1 occurs in the vicinity of DNA, probably at the kinetochore. This finding is consistent with the finding that Stu1 interacts with Slk19 in vivo (both proteins localize to the kinetochores prior to anaphase) and findings from two other studies, which showed that Stu1 interacts with centromeric DNA (Amaro et al., 2008) and that Stu1 preferentially associates with unattached kinetochores (Ortiz et al., 2009). Together with the finding that *stu1-5* is synthetic lethal with *bub1Δ and mad2Δ*, I hypothesize that Stu1 is involved in a parallel spindle assembly checkpoint that is concentrated specifically at unattached kinetochores. Further study of the role of Stu1 in satisfying the spindle assembly checkpoint and its function at unattached kinetochores could reveal one mechanism of how unattached kinetochores are sensed by the cell, which has remained elusive to date.

My Stu1 truncation analyses yielded some interesting insights into the potential function and essential nature of Stu1. The fact that more than 50% of the protein can be truncated at the C-terminus without a loss of cell viability indicates that most or all of Stu1's essential function is dependent on the first half of the protein, which contains the microtubule-binding domain and the TOG-like domains. The fact that cells with no visible Stu1 staining on microtubules during anaphase (*ase1Δ* and *stu1* truncation mutants) are viable suggests that the essential function may be dependent on the interaction between Stu1 and microtubules but that this interaction may be essential at the kinetochore-microtubule boundary but not at the spindle midzone.

My identification by mass spectrometry of an interaction between Stu1 and Slk19 is also an interesting finding. These proteins have not been suggested to interact by any previous study, but both proteins play important roles in anaphase. While the functional significance of this interaction is still unknown, there are some reasonable possibilities to explain these results. First, the fact that GFP-Stu1 is mislocalized in *slk19Δ* cells (greater concentration on kinetochores and lower concentration on midzone compared to wild type) indicates that Slk19 is responsible for relocalizing Stu1 from the kinetochores to the midzone upon anaphase onset. The relocalization of Slk19 itself is dependent on its cleavage by Esp1 (Sullivan et al., 2001). Given that Stu1 preferentially localizes to unattached kinetochores prior to anaphase onset (Ortiz et al., 2009), Esp1/Slk19 might be involved in the sensing of proper attachment and removal of Stu1 from a newly attached kinetochore. Another possibility is that Stu1 and Slk19 act together at the kinetochore as a complex that senses the lack of attachment of kinetochores to microtubules until Esp1 acts to remove both proteins at the proper time. An investigation of whether Slk19 also preferentially associates with unattached kinetochores would be necessary to answer this question.

In conclusion, my investigation of Stu1 has shown that this protein interacts with a number of other proteins, including Slk19, which is itself involved in anaphase progression, and a number of DNA-interacting proteins, perhaps as a result of its function at kinetochores. *STU1* also has genetic interactions with a specific subset of genes involved in the spindle assembly checkpoint. These data indicate that Stu1 might be functioning as a microtubule midzone stabilizer during anaphase but also that Stu1 possesses some currently unknown function at kinetochores, possibly related to the sensing of unattached kinetochores. Given its essential function and the requirement for its N-terminus for viability, Stu1 is likely to possess a novel function at kinetochores that is dependent on its interaction with microtubules.

2.4 Materials and Methods

Yeast culture

All yeast strains were cultured in standard YPD medium for growth, protein expression and cloning experiments, unless stated otherwise.

Phosphomutant generation

Point mutants were generated by first cloning a fragment of the STU1 gene containing the nucleotides of interest into a pBSKII vector (Stratagene). A KanMX6 marker (provided by K. Weis, UC Berkeley) was inserted into the 3'UTR of the STU1 sequence on the plasmid to facilitate genetic crosses. This plasmid was named pSTU1. Point mutations were introduced using the QuikChange Mutagenesis kit (Qiagen) and forward and reverse primers corresponding to the desired mutations (changing S1167 to A1167 or D1167 in Stu1). The STU1 sequence containing the mutation and KanMX6 sequence were amplified by PCR, gel purified and transformed into wild type diploid yeast using a standard lithium acetate transformation protocol (adapted from Schiestl et al., 1989). Clones that were resistant to geneticin (Gibco) were picked and sequenced to confirm their identity. These verified diploid cells were then sporulated to generate haploid mutants for analysis.

Western blotting

For western blotting experiments, proteins were either harvested from whole cell extracts using TCA precipitation with 15% trichloroacetic acid or immunoprecipitated from yeast using appropriate antibodies (mouse α-HA, 1:200; Roche, or rabbit α-GFP, 1:200; Torrey Pines). Proteins were denatured with sample buffer containing 5% β-mercaptoethanol and electrophoresed using SDS-PAGE. Proteins were transferred to nitrocellulose membranes using a wet transfer apparatus, and the membranes were blocked with 5% nonfat dry milk in TBS-T for 1 hour at 25^{o}C or overnight at 4^{o}C. The blots were incubated with primary antibodies (mouse α-HA 1:5,000 (12CA5, Roche) or rabbit α-GFP (1:2,000, Torrey Pines)) for 1 hour at 25^{o}C. Blots were washed for 45 minutes with TBS-T (50 mM Tris pH 7.4, 150 mM NaCl, 0.1% Tween-20) before being incubated with the appropriate secondary antibody (α-mouse or α-rabbit, 1:10,000; GE Healthcare) for 1 hour at 25^{o}C. Blots were washed again for 45 minutes in TBS-T before the proteins were visualized using ECL reagents (Thermo Scientific).

Stu1 protein purification

To purify Stu1 protein from yeast, first, a Stu1 overexpression plasmid was generated. The STU1 gene was cloned into the pRS426 expression plasmid that contained the pGal promoter, a C-terminal myc epitope tag and the *URA3* selection gene. The resulting plasmid, named pStu1GAL, was transformed into wild type yeast. Stu1 protein expression was induced as described previously for galactose overexpression (adapted from Rodal et al., 2002). To determine the level of expression, whole cell extracts were generated. In

brief, the cell pellet was resuspended in 600 μL cold lysis buffer (50 mM Tris-HCl, pH 7.5, 150 mM NaCl, 5 mM EGTA, 5 mM EDTA, 1X protease inhibitor IV (Calbiochem)). The solution was sonicated 3 times for 10 seconds each time on ice. An equal volume of 300-μm glass beads were added, and the extract was bead beat for 10 minutes at 4°C. NP-40 was added to 1% of the liquid volume to break apart cell membranes. The extract was centrifuged at 13,000 rpm for 15 seconds to pellet cell fragments. The supernatant was transferred to a new Eppendorf tube and centrifuged at 14,000 for 10 minutes at 4°C. After removing the cleared supernatant and calculating the protein concentration using Bradford reagent (Bio-Rad), the extract was pre-cleared by incubating with 40 μL protein A sepharose slurry (GE Healthcare) for 30 minutes at 4°C. The slurry was pelleted by centrifugation at 3,000 rpm for 1 minute, and the supernatant was transferred to a new Eppendorf tube. The extract was incubated with 5 μL α-myc antibody (9E10 monoclonal) for 1 hour at 4 °C. Then, 40 μL protein A sepharose slurry was added to the extracts and incubated for 30 minutes at 4 °C. The sepharose beads were centrifuged at 3,000 rpm for 1 minute, the supernatant was removed, and the beads were incubated in 2X protein sample buffer for 10 minutes at 65°C. The level of Stu1 protein immunoprecipitated by the myc-conjugated beads was checked by western blot; however, no detectable Stu1 protein was immunoprecipitated.

Stu1 protein was purified using a baculovirus-based expression system (Invitrogen), according to the manufacturer's instructions, in SF9 insect cells. In brief, the STU1 gene was cloned into a baculovirus vector that contained an N-terminal 6xHis epitope tag. The baculovirus vector was used to infect SF9 insect cells to induce protein expression. The viral titer was optimized at 1:200 before proceeding with large-scale purification. The cells were infected with the appropriate concentration of baculovirus and incubated for 72 hours to allow maximum expression level before the cells were no longer viable. The cells were collected from plates by scraping and processed using a standard imidazole His purification protocol (Qiagen) with slight modifications.

Following imidazole purification of Stu1 protein, the eluted fractions were passed over a Superdex 200 gel filtration column (GE Healthcare) using standard buffer for insect cell purification (50 mM NaH_2PO_4, 300 mM NaCl, 10 mM imidazole, pH 8.0) with 10% glycerol. The eluted fractions were collected in 1.5-mL aliquots and either frozen or concentrated in a centricon (Pall Life Sciences) with a 100-kDa cutoff value and frozen for later analysis.

Live cell microscopy

For live cell microscopy analyses, cells were grown at in 2-mL cultures at 25°C or 30°C in YPD until they reached log phase growth (OD_{600} of 0.5-0.75). They were then centrifuged at 2,500 rpm for 2 minutes and resuspended in 2 mL imaging medium (synthetic yeast medium containing 2% glucose and all necessary amino acids except tryptophan) for 2 cell cycles (3-4 hours). The cells were then centrifuged at 2,500 rpm for 2 minutes and resuspended in 100 μL imaging medium. Glass cover slips were incubated with 0.2 mg/ml Concanavalin A (Con A) for 10 minutes. Excess Con A was washed away, and 50 μL of cells were pipetted onto the Con A spots to allow adherence for 10 minutes. Excess cells were washed away with imaging medium, the chamber was filled with 750 μL

imaging medium, and the cells were imaged using an Olympus IX71 or IX81 equipped with digital cameras. Images were processed using Metamorph (Molecular Devices) and ImageJ (open source; http://rsbweb.nih.gov/ij/) software packages.

Mass spectrometric analysis

For Stu1 purification from yeast for mass spectrometric analysis, the Stu1-TAP strain (Tandem Affinity Purification tag; S-tag, TEV cleavage site, ZZ tag; Cheeseman et al., 2001) strain was obtained from S. Westermann in the Drubin lab. To obtain sufficient starting material, 12 liters of asynchronously growing yeast expressing Stu1-TAP protein were grown to an approximate OD_{600} of 1.0 in YPD. Stu1-TAP was purified as described previously (Cheeseman et al., 2001), with the exception that CL-6B sepharose resin (Sigma) was used in place of Q sepharose resin, and all relevant steps were performed in the presence of 150 mM KCl. The final purified extract was eluted into a solution of 8 M urea (8 M urea, 50 mM Tris-HCl, pH 8.8). This eluate was divided into two aliquots, snap frozen in liquid nitrogen and stored at -80^{o}C until it was used for mass spectrometric analysis.

The mass spectrometric analyses were performed on the material in 8 M urea solution by the Yates lab at Scripps Research Institute. One aliquot was used for MUD-PIT peptide analysis (as described in Link et al., 1999), and the other aliquot was passed through a titanium dioxide column to enrich for phosphopeptides before being analyzed (as described in Cantin et al., 2007). The results were given as the number and identities of all amino acid sequences detected and their confidence scores.

Yeast two-hybrid assay

For the Stu1 yeast two-hybrid assay, bait plasmids were generated from the plasmid vector pODB2 (provided by T. Hazbun, Purdue University). The *STU1* gene (full-length with various amino acid linker regions or gene fragments) was cloned into the plasmid downstream of the Gal4 DNA-binding domain. The plasmid was then sent to Professor Stan Fields' group at the University of Washington for a large-scale genomic screen of interacting partners. The screen was performed in duplicate, and single and double hits were identified and compiled.

Generation of *STU1* truncation mutants

Stu1 truncation mutant proteins were generated using the Longtine method (Longtine et al., 1998). In brief, primers targeting the truncation site were generated. The Longtine GFP module was amplified from a plasmid by PCR, generating a linear fragment with homology to the STU1 3'UTR and the coding sequence corresponding to the truncation site. The fragment was integrated into wild type diploid yeast; successful integration resulted in a loss of the appropriate 3' *STU1* gene sequence. These integrants were sequenced and sporulated to generate haploid strains for analysis.

Chapter 3: Slk19 regulates the movement of Cdc14 from the nucleus to the cytoplasm at the end of anaphase in *Saccharomyces cerevisiae*

3.1 Introduction

In eukaryotic cells, mitosis occurs in several tightly coordinated stages to ensure high-fidelity chromosome segregation. Much of this regulation is controlled by cyclin-dependent kinases (CDKs) and their opposing phosphatases. In *Saccharomyces cerevisiae*, the sole CDK, Cdc28, is primarily opposed by the phosphatase Cdc14 during mitosis (Visintin et al., 1998). The balance between Cdc28 phosphorylation and Cdc14 dephosphorylation allows the microtubule-based spindle to elongate and chromosomes to separate during anaphase (Khmelinskii et al., 2007). These kinase and phosphatase activities also allow mitotic exit and cytokinesis (reviewed in Queralt and Uhlmann, 2008). Because of their critical importance for proper mitotic progression and chromosome segregation, the activities of these enzymes are regulated by a variety of mechanisms.

In *S. cerevisiae*, Cdc14 activity is controlled at two major stages during mitosis; it is initially controlled by the FEAR (CdcFourteen Early Anaphase Release) network during early-to-mid-anaphase and later controlled by the MEN (Mitotic Exit Network) during late anaphase and telophase (reviewed in Stegmeier and Amon, 2004). These pathways direct Cdc14 localization to the appropriate subcellular location at the appropriate time in mitosis. Prior to anaphase onset, Cdc14 is sequestered in the nucleolus by its binding partner Net1, where it is considered inactive (Shou et al., 1999). After anaphase onset, Esp1 (separase), Slk19 and Spo12, members of the FEAR pathway, promote the partial movement of Cdc14 from the nucleolus to the nucleus (Stegmeier and Amon, 2002), where it dephosphorylates Cdc28-phosphorylated nuclear protein substrates (Pereira and Schiebel, 2003; Woodbury and Morgan, 2007; Jin et al., 2008; Khmelinskii et al., 2009). Many of these target substrates are microtubule-associated proteins (MAPs) that are important for spindle elongation and stability (Khmelinskii et al., 2007). At the end of anaphase, MEN proteins (Tem1, Lte1, Bub2, Bfa1, Cdc15, Dbf2, Mob1, Cdc5, Cdc14) function together to promote the further release of Cdc14 from the nucleus to the cytoplasm, where it participates as part of the MEN to resolve mitosis and promote cytokinesis (Visintin et al., 1998). This feedback loop involving Cdc14 and the MEN is necessary for proper mitotic exit.

While most, if not all, of the proteins that make up the FEAR and MEN pathways have been identified, the specific roles that these proteins play in Cdc14 regulation are only beginning to be understood. For example, it was recently shown that the kinase Dbf2, a MEN component, directly phosphorylates Cdc14, which promotes its release from the nucleus to the cytoplasm (Mohl et al., 2009). Cdc14 dephosphorylates Mob1, the binding partner of Dbf2, as part of a MEN feedback loop (Konig et al., 2010). Esp1 and its binding partner Slk19 play an important role in the FEAR pathway by facilitating the release of Cdc14 from the nucleolus to the nucleus, and full or partial deletion of SLK19 results in a moderate defect in Cdc14 release to the nucleus (Stegmeier et al., 2002), but the precise roles of these proteins in Cdc14 regulation is unknown.

SLK19 was first identified as a gene that is synthetic lethal with *KAR3*, and deletion of *SLK19* causes defects in spindle stability and chromosome segregation (Zeng et al., 1999). Sullivan et al. (2001) found that Slk19 is a proteolytic substrate of Esp1; a

subsequent study identified both Slk19 and Esp1 as members of the FEAR pathway (Stegmeier et al., 2002). It is unclear whether these two functions of Slk19, spindle stability and Cdc14 regulation, are different aspects of a single function or are independent functions. A recent *SLK19* gene truncation analysis suggested that these two functions are independent and require different regions of Slk19 (Havens et al., 2010), but it is possible that these seemingly separate functions are distinct manifestations of a single upstream regulatory mechanism. These two functions may be separated by differences in the post-translational modification state of Slk19, differences in its protein binding partners or differences in its localization pattern. As discussed in Chapter 2, I found that Slk19 interacts physically with the MAP Stu1, suggesting a complex but poorly understood interaction between FEAR function and mitotic spindle stability. I wanted to study this potential link between Cdc14 regulation and spindle stability through the function of Slk19 during anaphase.

Some of the most important regulatory mechanisms of anaphase progression involve post-translational modifications of proteins. Sumoylation is a post-translational modification that is analogous to ubiquitination. Sumoylation is the process of covalently attaching the SUMO (Small Ubiquitin-like MOdifier) protein (Smt3 in *S. cerevisiae*) to specific lysine residues of target substrates. While the effects of sumoylation of substrate proteins are poorly understood and appear to vary from substrate to substrate, several studies have found roles for sumoylation of mitotic proteins in *S. cerevisiae*, including Ndc10, Bir1, Cep3, Ndc80 (Montpetit et al., 2006), Kar9 (Leisner et al., 2008) and septin proteins (Johnson and Blobel, 1999). Furthermore, temperature-sensitive mutants of the SUMO-conjugating enzyme Ubc9 and the SUMO isopeptidase Ulp1 cause arrest at the metaphase-to-anaphase transition, with short spindles and undivided DNA (Seufert et al., 1995; Li and Hochstrasser, 1999).

There are several lines of evidence suggesting that Slk19 is sumoylated in vivo. First, Slk19 was identified as potentially sumoylated in a large-scale sumoylation screen in *S. cerevisiae* (Denison et al., 2005). In work from my lab, Slk19 was also found to interact with the SUMO-conjugating enzyme Ubc9 by yeast two-hybrid analysis (Wong et al., 2007); Ubc9 is an interaction partner that is known to be related to in vivo sumoylation (Müller et al., 2001). Therefore, I sought to determine whether Slk19 is sumoylated in vivo and, if so, to determine the effect of this post-translational modification on Cdc14 regulation.

My research results, to be explained in detail in the following pages, demonstrated that Slk19 is indeed sumoylated in vivo. Moreover, Slk19 mutants that have decreased sumoylation (Slk193R) present defects in the timing of Cdc14 localization from the nucleus to the cytoplasm; these mutants cause Cdc14 to be prematurely localized to the cytoplasm prior to spindle disassembly. This premature movement might be related to a change in the physical interaction between Slk19 and Dbf2 kinase, a MEN component. The consequence of this premature localization of Cdc14 is inappropriate activation of the MEN, as Slk193R partially rescues a temperature-sensitive allele of the MEN kinase Cdc15. Slk193R also displays defects in spindle elongation; mutants lose the distinction between the fast and slow phases of anaphase, and the overall spindle elongation time is decreased compared to wild type. I conclude that sumoylated Slk19 is important for regulating the localization of Cdc14 from the nucleus to the cytoplasm at the end of anaphase and that Cdc14 release to the cytoplasm is the primary regulator of mitotic exit.

3.2 Results

Slk19 is sumoylated in vivo

To determine whether Slk19 is sumoylated in vivo, I constructed a Slk19 protein that contains 13 repeated c-myc sequences (EQKLISEEDL) fused to the C-terminus of the Slk19 protein and expressed in yeast cells. I then immunoprecipitated (IP) Slk19-13xMyc from yeast cell extracts and probed for Smt3 (SUMO) by western blot. I found that sumoylated Slk19 was virtually undetectable in asynchronously growing cells but was enriched in cells that were arrested with 0.1 M hydroxyurea (HU) (Figure 9). This finding indicates that sumoylated Slk19 is present at high levels between the end of S phase and approximately the point of the metaphase-to-anaphase transition. Little or no sumoylated Slk19 was detected in late anaphase cells that were arrested with 0.1 M HU and then released into anaphase, indicating that the Slk19 sumoylation status changes during mitosis and decreases to steady-state levels by the end of anaphase.

In addition to detecting sumoylated Slk19 by IP, I also assessed the sumoylation status of Slk19 directly by mass spectrometry. Wild type Slk19-TAP (tandem affinity purification tag) was purified from yeast and assessed using the MALDI-TOF method (Link et al., 1999). The results of the mass spectrometric analysis are listed in Supplemental Table 1. The Smt3 amino acid fragment EQIGG, which is the C-terminal fragment of Smt3 that remains covalently linked to target lysine residues after trypsin digest was detected on lysine 449 (K449) of Slk19 in asynchronous cells. In addition, Smt3 was detected as a Slk19-interacting partner, supporting the finding of sumoylation of Slk19. The finding of a single sumoylated lysine in unsynchronized cells is in agreement with the low level of sumoylation detected in unsynchronized cells by IP. Based on these mass spectrometry and IP results, I conclude that Slk19 is sumoylated in vivo, but that the steady-state level of sumoylation is low.

Growth and expression phenotypes of Slk19 sumoylation mutants

To understand the effects of sumoylated Slk19 on mitotic progression, I mutated putative sumoylated lysine residues of Slk19 and assessed the phenotypes of the lysine point mutants. I first analyzed the Slk19 protein sequence to identify residues that were likely to be sumoylated. To do this, I used an optimized sumoylation clustering consensus sequence, [IVQM][K][X][DE] (developed in my lab by Aldaz et al., submitted), a modification of the currently accepted consensus sequence of [ILV][K][X][DE] (Bernier-Villamor et al., 2002). This approach identified five lysine residues in Slk19 that match the consensus sequence (Figure 10A). I mutated these lysines, individually and in combination, to arginines to prevent sumoylation, created fusions of resultant proteins with C-terminal epitope tags and assessed the mutant phenotypes of cell growth and protein expression.

None of the single or combination K-to-R mutants presented bulk growth defects on plates or in culture (data not shown). With regard to protein molecular weight and expression level, no single mutant had an apparent molecular weight or protein expression level that differed from wild type Slk19 (Figures 10B and C). However, the Slk19 mutant with the consensus lysines K412, K440 and K524 mutated to arginine ($Slk19^{3R}$) and the mutant with all five consensus lysines mutated to arginines ($Slk19^{5R}$) had slightly lower

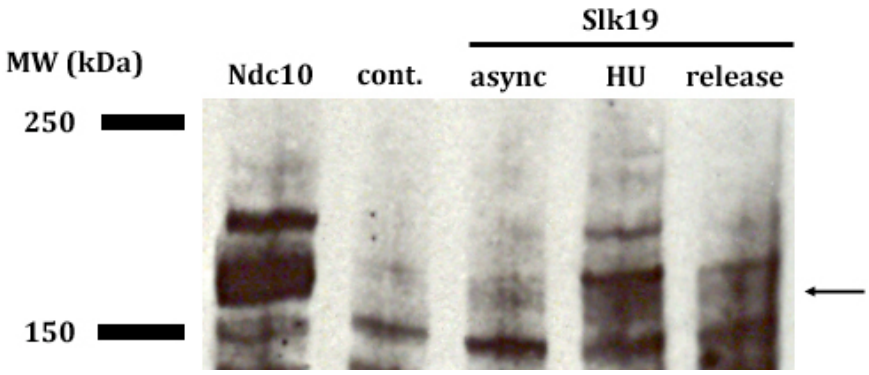

Figure 9. Slk19 is sumoylated in vivo. Western blot, probed with α-Smt3 antibody, of Myc-tagged sumoylated proteins immunoprecipitated with α-Myc antibody. From left, lanes represent Ndc10-13xMyc cells grown asynchronously (positive control), wild type cells with no Myc-tagged protein, grown asynchronously (negative control), Slk19-13xMyc cells grown asynchronously, Slk19-13xMyc cells arrested with 0.1 M hydroxyurea (HU) and Slk19-13xMyc cells arrested with 0.1 M HU and released into anaphase for 75 minutes before harvest. For both Ndc10-13xMyc and Slk19-13xMyc, the sumoylated species have large apparent molecular weights than the corresponding non-sumoylated proteins. Sumoylated Slk19 is indicated by the arrow.

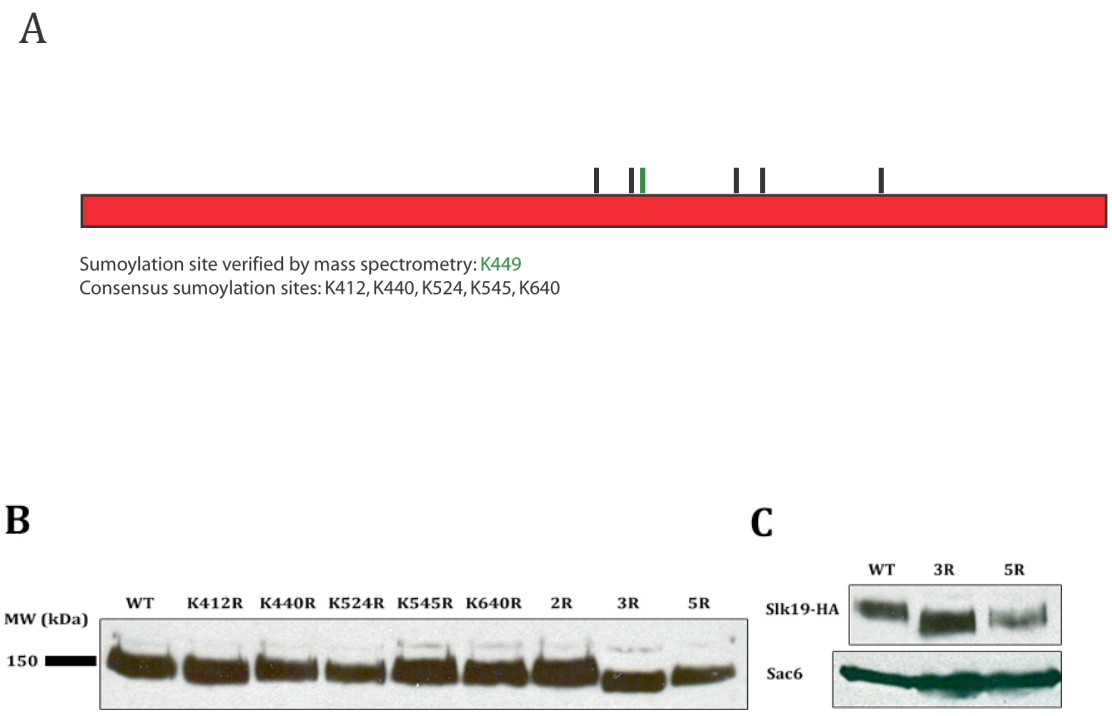

Figure 10. Slk19 combination sumoylation mutants have smaller apparent sizes than wild type Slk19. Western blots of Slk19-3xHA proteins from whole-cell extracts. Blots probed with α-HA antibody. (A) Lanes, from left: wild type Slk19, Slk19 (K412R), Slk19 (K440R), Slk19 (K524R), Slk19 (K545R), Slk19 (K640R), Slk19 (K412R K440R; 2R), Slk19 (K412R K440R K524R; 3R), Slk19 (K412R K440R K524R K545R K640R; 5R). (B) Lanes, from left: wild type Slk19, $Slk19^{3R}$, $Slk19^{5R}$. Sac6 was used as a loading control. This western blot highlights the differences in apparent molecular weight and expression level of $Slk19^{3R}$ and $Slk19^{5R}$ compared to wild type Slk19.

apparent molecular weights than wild type Slk19 (approximately 140 kDA for the two mutants vs. approximately 145 kDA for wild type Slk19). In addition, Slk19^{5R} had a protein expression level that was approximately 50% of the expression levels of either wild type Slk19 or Slk19^{3R}. Subsequent investigation demonstrated that Slk19^{5R} and Slk19^{3R} had identical phenotypes, so to prevent potential off-target effects of decreased protein expression, all experiments were performed with Slk19^{3R}.

In addition to assessing the protein expression levels of the Slk19 sumoylation mutants, I also assessed their sumoylation status. Using HU arrest and IP western protocols, I found that Slk19^{3R} and Slk19^{5R} are still sumoylated in vivo but that their sumoylation patterns differ from those of wild type Slk19. In particular, the band representing sumoylation is much more diffuse and appears to be running at a lower apparent molecular weight in the Slk19^{3R} and Slk19^{5R} mutants compared to wild type (Figure 11). This finding indicates that while I have not eliminated all sumoylated lysines on Slk19, the lysines that were mutated have the effect of decreasing the overall sumoylation of the protein. Given that the mass spectrometric analysis identified an additional sumoylated lysine, K449, I am currently mutating that lysine residue to arginine and will assess the sumoylation status of this *slk19* mutant.

Sumoylation mutants of Slk19 have defects in spindle elongation

After evaluating the growth and expression characteristics of the Slk19 sumoylation mutants, I sought to understand the effects of decreased sumoylation on the known functions of Slk19. I first analyzed the localization pattern of Slk193R compared to wild type Slk19. Wild type Slk19 localizes to the kinetochores prior to the activation of the Anaphase-Promoting Complex/Cyclosome (APC/C); upon activation of the APC/C, Esp1, the binding partner of Slk19, cleaves Slk19 between amino acids 77 and 78, and the C-terminal fragment localizes to a focused region of the spindle midzone (Sullivan et al., 2001). Thus, during anaphase, Slk19 is present at both the kinetochores and the spindle midzone. In mid-to-late anaphase, prior to spindle disassembly, the midzone localization of Slk19 disappears, leaving only two Slk19 spots, one at each kinetochore cluster.

To assess the localization of wild type Slk19 and Slk19^{3R} sumoylation mutant proteins, I created Slk19-GFP and Slk19^{3R}-GFP fusions integrated at the endogenous *SLK19* locus. Wild type Slk19-GFP had the characteristic Slk19 localization pattern (Figure 12A). Slk19^{3R}-GFP also localized to the kinetochores and spindle midzone, but its localization at the midzone was aberrant. Instead of being tightly focused at the spindle midzone, the midzone signal was more diffuse than the wild type signal (Figure 12B). Similar defects in the focusing of the spindle midzone component Ase1 have been observed in the absence of *SLK19* and *ESP1* (Khmelinskii et al., 2007). This result suggests that Slk19^{3R} might cause defects in spindle midzone organization, which could lead to defects in spindle dynamics during anaphase.

Slk19 is known to be important for spindle stability and spindle midzone organization (Zeng et al., 1999; Khmelinskii et al., 2007), so because of the aberrant Slk19^{3R} midzone localization signal, I asked whether defects in Slk19 sumoylation had an effect on spindle dynamics. Unlike the phenotype seen in *slk19Δ* cells, in which spindles are prone to

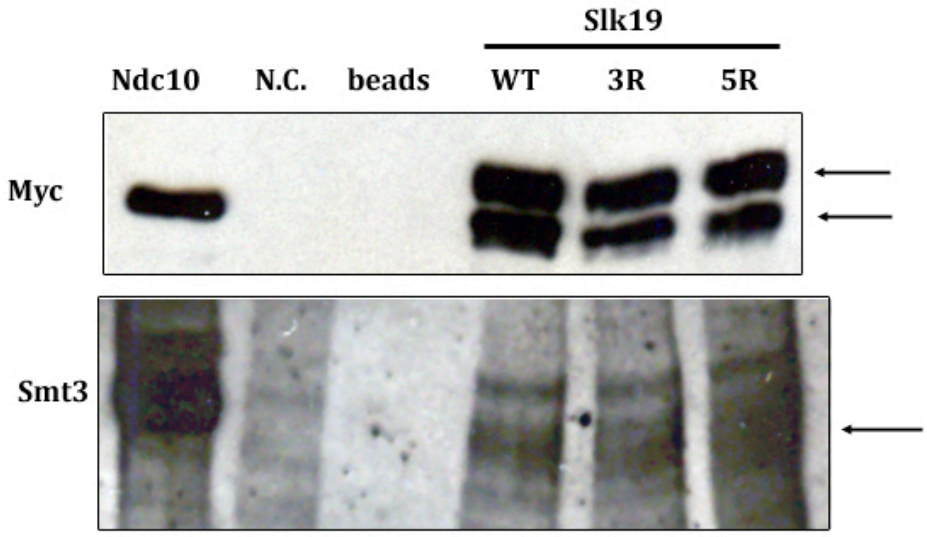

Figure 11. Slk19 sumoylation pattern is altered in Slk19^{3R} and Slk19^{5R} mutants. Western blots of Ndc10-13xMyc, 904 (negative control) cells, sepharose beads only, Slk19-13xMyc, Slk19^{3R}-13xMyc and Slk19^{5R}-13xMyc immunoprecipitated with α-myc 9E10 antibody. Cells were harvested after arrest with 0.1 M HU for 3 hours. Top blot shows myc input lanes. Bottom blot shows sumoylated species visualized with α-Smt3 antibody. "N.C." indicates negative control cells with no myc-tagged protein; "beads" indicates myc-conjugated sepharose beads that were not incubated with cell extract.

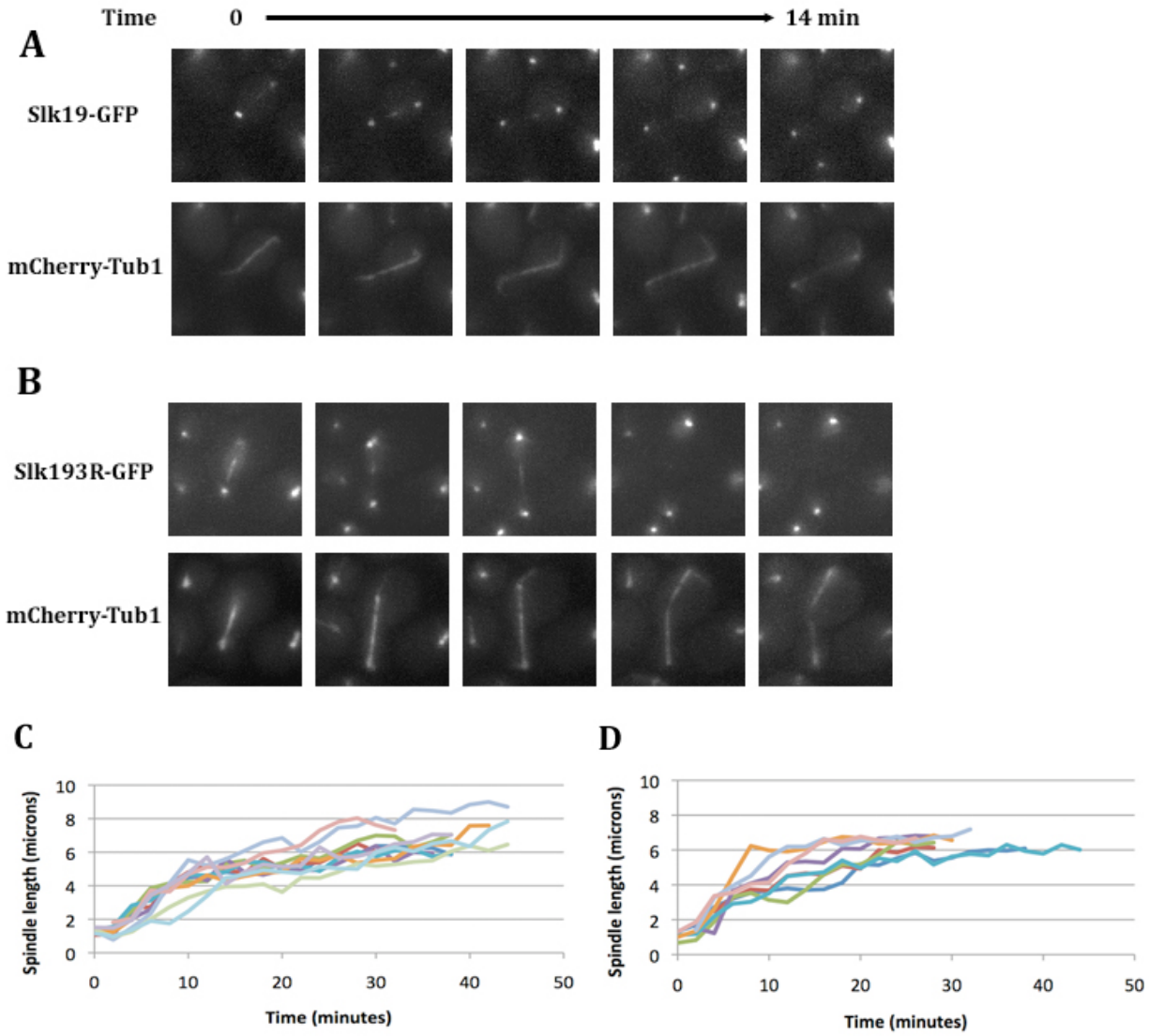

Figure 12. Slk19^{3R} has an altered localization pattern and causes cells to lose the transition between the fast and slow phases of anaphase. Live cell microscopy time course montages of endogenous fusion proteins (A) Slk19-GFP and (B) Slk19^{3R}-GFP. Microtubules are visualized with mCherry-Tub1, inserted at the URA3 locus. Anaphase spindle length traces of (C) Slk19 WT and (D) Slk19^{3R} are represented by colored lines. Each line represents an individual spindle.

breakage and often do not reach the mother and bud cell cortices before disassembling (Zeng et al., 1999), Slk19^{3R} cells did not have fragile spindles, and their spindles were able to reach slightly longer maximum lengths than wild type cells (7.05 μm for wild type Slk19 vs. 7.54 μm for Slk19^{3R}; p=0.002). Instead, Slk19^{3R} cells lost the transition between the fast and slow phases of anaphase; the fast phase is thought to represent the initial sliding of the two halves of the short spindle, and the slow phase is thought to represent microtubule polymerization at the plus ends of the two spindle halves (Kahana et al., 1995). Spindles in Slk19^{3R} cells either rapidly elongate to a normal final length, remaining at this length until disassembly, or elongate at a relatively steady rate throughout anaphase, with no division between the fast and slow phases (Figures 12C and D). These findings demonstrate that a defect in Slk19 sumoylation leads to defects in spindle elongation dynamics but not to loss of spindle stability.

Defects in Slk19 sumoylation cause defects in Cdc14 localization dynamics

As noted above, Slk19 is involved in spindle elongation as well as the FEAR pathway, processes that both involve the phosphatase Cdc14. Phosphorylation and dephosphorylation of a number of midzone components by Cdc28 and Cdc14, respectively, regulate spindle dynamics. Because of this dependence of phosphorylation and dephosphorylation on anaphase progression, and because *slk19D* mutants have defects in the release of Cdc14 from the nucleolus to the nucleus, I wanted to investigate whether a defect in Slk19 sumoylation has an effect on Cdc14 activity. First, I asked whether Slk19^{3R}, like *slk19D*, has an effect on the characteristic localization pattern of Cdc14. I found that, unlike *slk19D*, Slk19^{3R} has no defect in Ccd14 release from the nucleolus to the nucleus (data not shown). However, these cells do have a defect in the timing of Cdc14 release from the nucleus to the cytoplasm at the end of anaphase. In wild type cells, the appearance of Cdc14 at the bud neck (indicating its movement to the cytoplasm) is tightly coupled to spindle disassembly because the MEN is responsible for both Cdc14 release to the cytoplasm and spindle disassembly (reviewed in D'Amours and Amon, 2004). I found that in wild type cells, Cdc14 appearance at the bud neck occurred nearly concomitant with spindle disassembly, at an average time of 1.75 minutes after spindle disassembly. In Slk19^{3R} mutants, however, Cdc14 appeared at the bud neck prematurely, at an average time of 5.73 minutes *prior* to spindle disassembly, indicating that when Slk19 sumoylation is defective, Cdc14 release to the cytoplasm occurs prematurely (Figure 13A and B). The MEN component Dbf2 kinase has recently been shown to be involved in the localization of Cdc14 from the nucleus to the bud neck (Mohl et al., 2009). In my mass spectrometric analysis of wild type Slk19, I identified a possible Slk19-Dbf2 interaction (Supplemental Table 2). These findings suggest that sumoylated Slk19 plays a major role in restricting Cdc14 to the nucleus during anaphase, possibly through an interaction with Dbf2.

It is possible that this defect in the timing of Cdc14 release to the bud neck is simply due to a defect in anaphase spindle dynamics, as Slk19^{3R} mutants cause defects in the kinetics of spindle elongation. To eliminate this possibility, I assessed the change in localization of Cdc14 from the nucleus to the bud neck in an *ase1D* strain, a strain in which spindle dynamics are also aberrant (Schuyler et al., 2003). In these cells, however, Cdc14 moves from the nucleus to the bud neck with timing that not statistically significantly

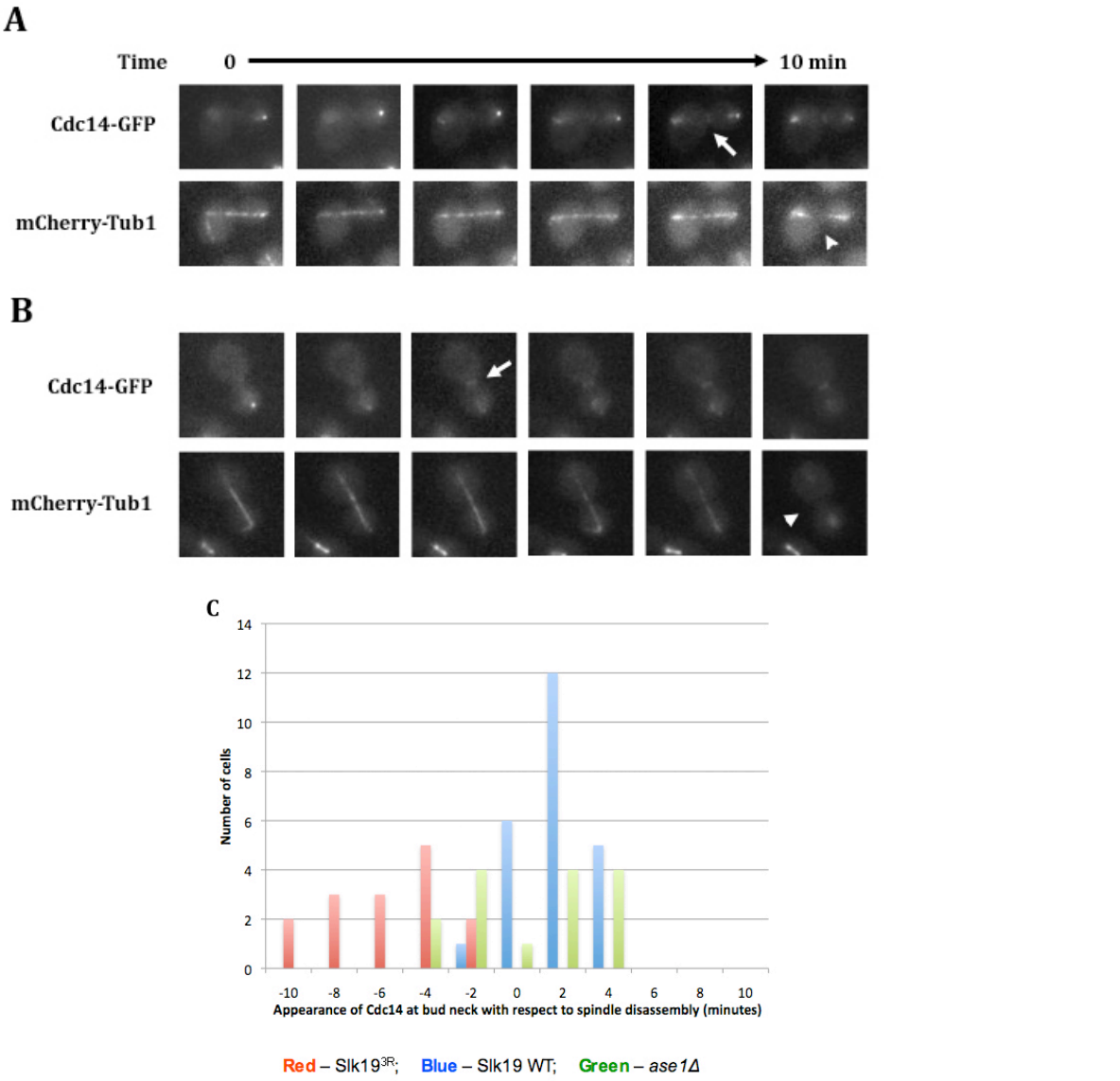

Figure 13. Slk19^{3R} causes premature localization of Cdc14 from the nucleus to the cytoplasm at the end of anaphase. Live cell microscopy time course montages of Cdc14-GFP and mCherry-Tub1 in (A) Slk19 WT and (B) Slk19^{3R} cells. The appearance of Cdc14-GFP at the bud neck is indicated with arrows, and spindle disassembly is indicated with arrowheads. (C) graph of the timing of Cdc14 appearance at the bud neck with respect to spindle disassembly. The bars indicate the number of cells in which Cdc14 appears at the bud neck at each 2-minute period pre- and post-disassembly (red = Slk19^{3R}, blue = Slk19 WT, green = *ase1Δ*).

different from wild type Slk19 cells (Figure 13C). This finding indicates that Cdc14 localization from the nucleus to the bud neck is decoupled specifically in Slk19^{3R} strains, and this premature localization is not due to a general defect in anaphase spindle dynamics.

Defects in Slk19 sumoylation partially rescue a temperature-sensitive MEN mutant

After determining that a defect in Slk19 sumoylation results in the premature release of Cdc14 to the cytoplasm, I investigated the downstream effect of such a defect in the timing of Cdc14 localization. Cdc14 is released from the nucleus to the cytoplasm through the actions of MEN proteins; once it reaches the cytoplasm, Cdc14 participates as a member of the MEN to promote mitotic exit (D'Amours and Amon, 2004). To understand whether premature release of Cdc14 to the cytoplasm has an effect on mitotic exit, we assessed the ability of Slk19^{3R} to suppress the late anaphase arrest phenotype of *cdc15-2*. The essential kinase Cdc15 is an integral component of the MEN, and at the restrictive temperature, *cdc15-2* mutants arrest at the end of anaphase with fully elongated spindles, strongly delaying or preventing spindle disassembly (Schweitzer and Philippsen, 1991). I compared the spindle disassembly defects (defined as the time between the spindle reaching its maximum length and the spindle disassembling) of *cdc15-2* cells in the genetic background of *SLK19*, *SLK19*^{3R} or *slk19Δ*. As shown in Figure 6, *SLK19 cdc15-2* cells showed a significant delay in spindle disassembly at 37°C compared to 25°C (average delay of 20.4 minutes; $p < 0.01$). However, this defect was rescued in *SLK19*^{3R} *cdc15-2* cells, which underwent spindle disassembly with minimal delay (average delay of 4.9 minutes; $p = 0.31$); this difference in delay times is statistically significant ($p < 0.01$). This rescue of delayed spindle disassembly did not occur in *slk19Δ cdc15-2* cells (average delay of 23.8 minutes; $p < 0.01$), indicating that this effect is not simply due to a loss of Slk19 protein function. These findings indicate that by allowing the premature movement of Cdc14 to the cytoplasm, Slk19^{3R} allows mitotic exit to proceed under conditions of decreased MEN function.

3.3 Discussion

Slk19 is known to play a role in Cdc14 release to the nucleus as a member of the FEAR network (Stegmeier and Amon, 2002), but its role in other aspects of Cdc14 regulation was previously unknown. Sumoylation has been identified as a post-translational modification of a number of proteins that play roles in mitotic progression, but the effects of sumoylation on Cdc14 regulation was also previously unknown. In this study, I found that Slk19 is sumoylated in vivo and that sumoylation of Slk19 is important for the regulation of Cdc14 localization between the nucleus and the cytoplasm in late anaphase.

In wild type cells, Cdc14 appears in the cytoplasm at the bud neck concomitant with spindle disassembly, owing to the fact that both Cdc14 release from the nucleus and spindle disassembly are controlled by the MEN (reviewed in D'Amours and Amon, 2004; Sullivan and Morgan, 2007). However, in cells in which Slk19 cannot be properly sumoylated, Cdc14 release from the nucleus is no longer coupled to spindle disassembly, allowing premature Cdc14 localization to the cytoplasm while the spindle is still intact. This premature localization of Cdc14 to the cytoplasm leads to aberrant MEN function. These results suggest that the primary function of the MEN is to release Cdc14 from the nucleus to the cytoplasm at the appropriate point in mitosis, and Cdc14 in the cytoplasm is the main effector of mitotic exit.

Cdc14 dephosphorylates two components of the MEN, the kinase Cdc15, and the Dbf2 kinase-regulator Mob1 (Jaspersen and Morgan, 2000; Konig et al., 2010). These dephosphorylation events are part of a positive feedback loop that is necessary for mitotic exit. While this positive feedback loop does seem to be occurring during mitotic exit, the results of the present study, wherein premature localization of Cdc14 to the cytoplasm rescues a *cdc15-2*-mediated defect in spindle disassembly, suggest a predominant role for Cdc14 in mitotic exit. This idea is supported by a recent report by Mohl et al. (2009), which demonstrated that Cdc14 is directly phosphorylated by Dbf2 kinase, a MEN component, on its nuclear localization signal, allowing Cdc14 to be released from the nucleus into the cytoplasm.

In addition to demonstrating the effects of inappropriate localization of Cdc14 to the cytoplasm, this study introduces a novel mechanism of cross talk between the FEAR and MEN pathways. Previous studies have shown that Polo-like kinase (Cdc5 in *S. cerevisiae*) plays roles in both the FEAR and MEN pathways (Lee et al., 2001; Manzoni et al., 2010). Slk19 physically interacts with Cdc5 (Rahal and Amon, 2008), so the phosphorylation status of Slk19 might affect its sumoylation and vice versa, further linking the FEAR and MEN pathways. Slk19 seems to restrict Cdc14 localization to the nucleus during FEAR and prior to MEN onset, indicating a broader role for Slk19 regulation of Cdc14 localization and a more complex relationship between FEAR and MEN than was previously appreciated.

The results of this study show that Slk19, a member of the FEAR pathway that was previously only known to regulate the movement of Cdc14 from the nucleolus to the nucleus, also plays a role in retaining Cdc14 in the nucleus throughout anaphase. It is possible that sumoylated Slk19 cooperates with its FEAR partner Esp1 to retain Cdc14 in the nucleus until mitotic exit. However, given the fact that Esp1 leaves the spindle midzone significantly earlier in anaphase than does Slk19 (Khmelinskii et al., 2007), it is unlikely that Esp1 is a constitutive binding partner of Slk19 or that Esp1 participates in this late

anaphase function of Slk19. Future studies regarding the cell-cycle dependence of the Slk19-Esp1 interaction and the effect of a loss of Slk19-Esp1 interaction on Cdc14 localization would be necessary to answer this question.

Another possibility for the mechanism of action of Slk19 on Cdc14 localization is an interaction with Dbf2 kinase, which is responsible for phosphorylating and presumably inactivating the nuclear localization signal of Cdc14 at the end of anaphase. This possibility is made more likely by the fact that I identified Dbf2 as a potential Slk19-interacting protein by mass spectrometry. One possible explanation is that sumoylated Slk19 interacts with Dbf2 and inhibits the interaction between Cdc14 and Dbf2, preventing the inactivation of the nuclear localization signal on Cdc14 until the appropriate point in mitosis. In this case, even with a $Slk19^{3R}$ mutant, the loss of Dbf2 would still prevent Cdc14 movement to the bud neck during mitotic exit. However, there might be a cell cycle-dependent decrease in the affinity of Dbf2 for Cdc14 or Slk19 in $Slk19^{3R}$ mutant cells. Alternatively, a defect in Slk19 sumoylation could somehow bypass the requirement for Dbf2 in Cdc14 release from the nucleus. In this case, with a $Slk19^{3R}$ mutant, the loss of Dbf2 would have little or no effect on Cdc14 localization to the bud neck at the end of anaphase.

In conclusion, I have identified a novel mechanism of Cdc14 regulation that involves a member of the early anaphase release network, Slk19, but regulates Cdc14 localization at the end of anaphase. This regulation may also involve an interaction between Slk19 and the MEN kinase Dbf2. These findings suggest that the cross talk between FEAR and MEN is extensive and involves more members of both pathways. In addition, the findings of this study implicate sumoylation in the regulation of anaphase dynamics through Cdc14 localization, opening a new avenue of research into the regulation of anaphase progression through the sumoylation of mitotic substrates.

3.4 Materials and Methods

Yeast culture

Yeast were grown in standard rich medium (YPD) at 30˚C for mutagenesis, immunoprecipitation and protein expression experiments. For hydroxyurea (HU) arrest experiments, yeast were grown in YPD at 30˚C until they reached an OD_{600} of 0.5-0.7, at which time HU (Sigma) was added to a final concentration of 0.1 M. The cells were incubated for three hours in 0.1 M HU, spun down, washed with ddH_2O and either collected immediately and snap frozen in liquid nitrogen or released into YPD without HU, grown for 75 minutes and collected and snap frozen in liquid nitrogen for later use.

Immunoprecipitation and western blot

For immunoprecipitation and western blotting experiments, cells were grown under standard conditions, washed with ddH_2O, snap frozen in liquid nitrogen and stored at -80˚C for later use. Myc immunoprecipitation experiments were performed as described previously (Montpetit et al., 2006) with some modifications. After extracts of total cellular protein were prepared, they were precleared for 30 minutes at 4˚C with protein G sepharose (40 μL) before incubation with 5 μL of anti-Myc antibody (9E10 clone) for 1 hour at 4˚C. After this incubation period, 50 μL protein G sepharose was added to each sample, and the suspensions were incubated for 30 minutes at 4˚C. The sepharose was then washed three times with cold lysis buffer. All liquid was removed, 30 μL of 2X protein sample buffer was added, and the samples were incubated at 70˚C for 10 minutes before being loaded onto a 5% agarose gel for SDS-PAGE. The proteins were transferred to nitrocellulose membranes, blocked with TBS-T/5% skim milk and incubated with anti-Smt3 antibody (rabbit polyclonal, 1:2,000, provided by P. Hieter, or rabbit polyclonal, 1:10,000, provided by V. Guacci) for one hour at room temperature. The blots were washed with TBS-T for 45 minutes and incubated with an anti-rabbit secondary antibody (1:10,000) for 45 minutes at room temperature. After washing the blots again with TBS-T for 45 minutes, protein bands were visualized with SuperSignal West ECL reagents (Thermo Scientific).

Live cell microscopy

For standard microscopy experiments, cultures were grown in imaging medium (synthetic medium with 2% glucose and required amino acids minus tryptophan) at 25˚C until they reached mid-log phase. They were pelleted and resuspended in 100 μL of imaging medium. Imaging chambers were prepared by adding 0.2 mg/mL concanavalin A (Con A) to round glass cover slips and incubating at room temperature for 10 minutes. Excess Con A was washed off with imaging medium, and 50 μL of cell suspension was spotted onto each cover slip. The cover slips were incubated for 10 minutes to allow cell adherence and then mounted in a custom ring apparatus, the chamber of which was filled with imaging medium. Cells were imaged on an Olympus IX81 microscope at 2-minute intervals, taking 9 z-slices at 0.3 μm apart for each time point. Metamorph (Molecular

Devices) and ImageJ (open source; http://rsbweb.nih.gov/ij/) software programs were used for image capture and analysis, respectively.

For temperature-sensitive live cell microscopy experiments, cells were grown to mid-log phase in imaging medium at 25˚C. The cells were then shifted to the restrictive temperature (30˚C or 37˚C) for two hours. Then, the cells were washed with imaging medium at the appropriate temperature and mounted on Con A-coated round cover slips, which were incubated at the appropriate temperature for 10 minutes. The cover slips were mounted in the custom ring apparatus, which was filled with 500 μL imaging medium at the appropriate temperature. The cells were imaged on an Olympus IX81-OMAC microscope fitted with a temperature-controlled imaging chamber and captured and analyzed as described above.

TAP purification of Slk19 and mass spectrometric analysis

Slk19-TAP was purified as described previously (Cheeseman et al., 2001), with minor modifications. To purify HU-arrested Slk19-TAP, 12 L of cells were grown to OD_{600} 0.5-0.7 before being arrested for 3 hours with 0.1 M HU. Cells were then harvested, washed with ddH_2O and processed as described previously for TAP-tagged strains.

For mass spectrometric analysis of Slk19-TAP, purified protein was eluted into 8.0 M urea buffer (8.0 M urea, 50 mM Tris-HCl, pH 8.8), snap frozen in liquid nitrogen, and sent on dry ice to my collaborator, Professor John Yates (Scripps Research Institute), for analysis by MUD-PIT mass spectrometry (Link et al., 1999). The Smt3 fragment EQIGG was detected as an additional molecular weight species associated with substrate lysines.

Generation of Slk19 sumoylation point mutants

To generate missense point mutants in the *SLK19* coding sequence, the entire *SLK19* gene was amplified by PCR from wild type genomic DNA and cloned into a pBluescript vector, generating the pAFSLK19 plasmid. A 3xHA (marked with *KanMX6*) or 13xMyc (marked with *HIS3*) epitope tag was inserted in-frame with the *SLK19* gene into pAFSLK19. Single base pairs were mutated in pAFSLK19 using the QuikChange Mutagenesis kit (Qiagen). Mutations were verified by sequencing. The mutated *slk19* gene sequences were amplified by PCR, purified and transformed directly into wild type yeast. Putative genomic integrants were identified by selection on agar plates containing YPD+G418 or synthetic medium lacking histidine, genomic DNA sequencing and expression of the epitope-tagged Slk19 proteins by western blot.

Discussion, future directions and closing remarks

Studies in yeast have yielded numerous insights into common mechanisms of biological action of eukaryotic cells and will continue to provide a great deal of information applicable to metazoan cells and, ultimately, translational and medical research into human disease. The ease of performing genetic, cell biological and biochemical experiments in yeast to study the essential mechanisms of mitosis has allowed an increased understanding of a process that is extremely complicated to study in metazoans. My dissertation research has explored a large number of relationships among proteins involved in mitosis and has provided several paths of future study.

My investigation of the MAPs Slk19 and Stu1 has increased our understanding of the events that occur during the anaphase stage of mitosis. I have found that both proteins are post-translationally modified (Stu1 by phosphorylation and Slk19 by phosphorylation and sumoylation) and have a number of protein interaction partners, indicating a greater degree of interconnectedness among mitotic proteins than was known previously. These findings highlight the idea that seemingly unrelated processes during mitosis may be regulated in concert or by common mechanisms. For example, Stu1 and Slk19 physically interact in vivo, which introduces the possibility that spindle stability is linked to Cdc14 regulation through the joint activities of these two proteins. Moreover, the fact that both of these proteins are phosphorylated at residues that do not match known kinase consensus sites indicates that both spindle stability and the FEAR network may be regulated by a number of other kinases in addition to Cdc28. In vitro kinase assays with purified kinase, Stu1 and Slk19 proteins combined with an analysis of the effects of analog-sensitive mutant kinase alleles on Stu1 and Slk19 phosphorylation patterns might help to identify the kinase(s) responsible for Stu1 and Slk19 phosphorylation. One likely kinase candidate is the yeast Polo-like kinase, Cdc5. Cdc5 has only an imprecisely defined consensus sequence, and little is known about its kinase specificity. This kinase is known to play roles in a number of mitotic processes, however (reviewed in Lee et al., 2005), so it is reasonable to hypothesize that it might phosphorylate and regulate Stu1 and/or Slk19 in vivo.

My research into the function of Stu1 has increased our understanding of the signals that drive MAPs to the spindle midzone to aid in the maintenance of spindle stability. My findings that GFP-Stu1 is mislocalized in distinct ways in the absence of *ASE1* or *SLK19* indicate that Stu1 interacts with these two proteins in very different ways. In the absence of *ASE1*, Stu1 no longer localizes to the anaphase spindle but is localized in a diffuse nuclear pattern; it does not remain at the kinetochores during anaphase. In the absence of *SLK19*, however, the localization of Stu1 to the midzone is decreased but not eliminated, and its localization to the kinetochores is increased and maintained during anaphase, in contrast to the wild type condition, in which Stu1 completely moves from the kinetochores to the midzone during anaphase. Like Ase1, Stu1 and Slk19 may also be scaffold proteins involved in microtubule stabilization at the midzone; further investigation of the in vitro interactions among Slk19, Stu1 and microtubules are needed to answer such a question.

Regardless of their status as scaffold proteins, microtubule stabilizers or proteins that perform some other function at the midzone, these proteins' patterns of localization (particularly their patterns in mutant backgrounds) provide clues to their unique functions.

Stu1 and Slk19 localize to the kinetochores prior to anaphase onset, indicating some function at the kinetochore that is not shared by Ase1. Slk19, but not Ase1, seems to provide a signal for Stu1 to be released from the kinetochores upon anaphase onset. However, Ase1 provides a stronger signal than Slk19 for Stu1 to move to the midzone once anaphase has begun. Therefore, Stu1 depends on both Slk19 and Ase1 for its localization, but these requirements are distinct. One outstanding question is whether the converse is true; the evidence for Stu1's effect on Ase1 and Slk19 localization is scant. Khmelinskii et al. (2007) demonstrated that Ase1 still localizes to the midzone in a *stu1* knockdown degron allele, but this allele could retain some residual function, and the spindles are exceedingly short in this mutant, obscuring the true extent of Ase1 association with microtubules. These investigations are further complicated by the fact that Stu1 is essential, and its major visualized effect at the restrictive temperature is to prevent spindle elongation during anaphase (Yin et al., 2002). Live cell microscopy experiments of *stu1-5* and either Slk19-GFP or Ase1-GFP at fine temperature gradations (e.g., imaging cells from 30°C to 37°C at 1-degree increments) could provide insight into whether Stu1 is required for or affects Slk19 and/or Ase1 localization.

My dissertation research identified a physical interaction between Stu1 and Slk19. *STU1* and *SLK19* are not synthetic lethal with each other, indicating that they are probably functioning in the same pathway in vivo. Their patterns of protein localization, discussed previously, also suggest their interdependency in vivo. However, the difficulties in studying Stu1 directly have hampered my efforts to further explore the relationship between these two proteins. The inability to detect tagged or native Stu1 protein in whole-cell extracts has made it difficult to assess the cell cycle-dependent interactions between Stu1 and Slk19. The fact that Slk19 was not detected as a Stu1-interacting protein in a Y2H assay also made it difficult to determine which region of Stu1 is interacting with Slk19, which is necessary to specifically disrupt this interaction without abolishing Stu1 protein function. Because Stu1 has recently been shown to localize to unattached kinetochores (Ortiz et al., 2009), and Slk19 has been shown to regulate centromeric elasticity (Zhang et al., 2006), further investigation into the interaction between these two proteins prior to anaphase onset may yield novel kinetochore functions of this complex that are independent of their spindle stability and FEAR network functions, respectively.

My research, as well as findings from other studies, can provide insight into the function of Stu1 at the kinetochore. The fact that Stu1 localizes to unattached kinetochores and moves away from kinetochores once all proper attachments have been made (Ortiz et al., 2009) is consistent with a role in the spindle assembly checkpoint. *stu1-5* is strongly synthetic lethal with *bub1D*, indicating that while these two proteins are unlikely to function in the same pathway, they may function in parallel spindle assembly checkpoint pathways. Stu1 was also found to interact with Bub1 by Y2H (Wong et al., 2007), indicating that the two proteins are in close physical proximity at some point during the cell cycle, consistent with their shared localization at kinetochores. These findings lead to a hypothesis that Stu1 is functioning in a spindle assembly checkpoint pathway that is distinct from the pathway involving Bub1. Gaining a better understanding of these distinct pathways could lead to investigations about different types of improper attachments or spindle assembly checkpoint signals. Given the colocalization of Stu1 and Slk19 at kinetochores, this pathway may also involve Slk19.

Slk19 is known as a member of the FEAR (CdcFourteen Early Anaphase Release) network regulating Cdc14 localization during early anaphase (Stegmeier and Amon, 2002). My research, however, has added to the known role of Slk19 in anaphase by demonstrating that it also regulates Cdc14 localization during late anaphase, prior to mitotic exit. This regulation is dependent on sumoylation of Slk19, which has not been previously demonstrated for Slk19 or any regulator of Cdc14 function.

Mitotic exit and the interplay between members of the mitotic exit network (MEN) has become much more complicated in recent years, as a number of studies have demonstrated increasing levels of interdependency and mutual regulation in this pathway (Mohl et al., 2009, Konig et al., 2010). A more complete understanding of the regulation of mitotic exit will require the identification of all members of the pathway and their mechanisms of interaction. Future work that builds on my dissertation research would involve confirming the interaction between Slk19 and Dbf2 and determining whether Slk19 interacts with other members of the MEN in a Cdc14-dependent or –independent manner. Cell-cycle-dependent co-immunoprecipitation of pairwise interactions between members of the FEAR and MEN pathways, particularly Slk19, would be a logical step in understanding these relationships.

Another avenue of study that arises from my research would be to better understand the functional consequence of Cdc14 movement from the nucleus to the bud neck. Dephosphorylation of a number of Cdc14 target substrates might be tightly regulated with respect to spindle disassembly, and the Slk19 sumoylation mutant background could be an excellent method for determining whether a change in localization of Cdc14 changes the phosphorylation status of proteins involved in spindle elongation and/or mitotic exit.

In addition to gaining a deeper understanding of the regulatory interplay between Cdc14 localization and mitotic exit, my research also introduces the regulation of anaphase progression by sumoylation. A previous study demonstrated that a number of proteins with roles in anaphase are sumoylated in vivo (Montpetit et al., 2006), but the functional consequences of these sumoylation events are poorly understood. If sumoylation is a mechanism for regulating anaphase progression through Cdc14 function, then other members of the FEAR and/or MEN network might also be sumoylated in vivo. A combination of protein purification from yeast using the TAP tagging protocol that was used in this study and other studies from my lab and mass spectrometric analysis of sumoylated lysine residues (by searching for the SUMO modification peptide fragment EQIGG on substrate lysines) could identify a number of sumoylated proteins in vivo. As large-scale sumoylation studies have generally non-overlapping datasets, it seems clear that the detection of transient sumoylation events is difficult and may depend on unique conditions and arrested cell cycle states for each protein. It would be very interesting to arrest yeast cells at specific cell cycle stages, such as the G2/M transition, late anaphase and telophase, and use mass spectrometry to identify all sumoylated substrates in the proteins present in the arrested samples. In this way, similar to efforts that have been made by my lab and others to identify cell cycle-specific phosphorylation profiles, sumoylation profiles could be generated for specific stages of the cell cycle and for specific cellular environmental conditions.

Finally, an outstanding question that has arisen from my research is how sumoylation of Slk19 is regulating Cdc14 localization. I believe that additional investigation into the cell cycle dependency of sumoylation of Slk19 and the interplay between

sumoylation and phosphorylation of Slk19 will help to answer the question of the mechanism of action of sumoylation on Cdc14 regulation. In addition, a comprehensive analysis of the mutants (knockout or temperature sensitive) that exacerbate or rescue the phenotype of premature movement of Cdc14 to the bud neck will help to identify the other proteins that are involved in this regulatory process.

In conclusion, my dissertation research has increased our collective understanding of the protein-protein interactions that occur during mitosis, provided supporting evidence for the role of Stu1 as a kinetochore-interacting protein, introduced sumoylation as a mechanism for regulating Cdc14 function during anaphase and identified Slk19 as a protein that regulates Cdc14 localization during late anaphase and mitotic exit as well as early anaphase. My research has also generated a number of interesting questions with respect to the study of Stu1, Slk19 and anaphase progression.

References Cited

Akhmanova A, Hoogenraad CC, Drabek K, Stepanova T, Dortland B, Verkerk T, Vermeulen W, Burgering BM, De Zeeuw CI, Grosveld F, Galjart N. Clasps are CLIP-115 and -170 associating proteins involved in the regional regulation of microtubule dynamics in motile fibroblasts. Cell. 2001 Mar 23;104(6):923-35.

Akiyoshi B, Nelson CR, Ranish JA, Biggins S. Analysis of Ipl1-mediated phosphorylation of the Ndc80 kinetochore protein in Saccharomyces cerevisiae. Genetics. 2009 Dec;183(4):1591-5.

Al-Bassam J, Kim H, Brouhard G, van Oijen A, Harrison SC, Chang F. CLASP promotes microtubule rescue by recruiting tubulin dimers to the microtubule. Dev Cell. 2010 Aug 17;19(2):245-58.

Amaro IA, Costanzo M, Boone C, Huffaker TC (2008) The Saccharomyces cerevisiae Homolog of p24 Is Essential for Maintaining the Association of p150Glued With the Dynactin Complex. Genetics. 178(2):703-9.

Andrade MA, Perez-Iratxeta C, Ponting CP. Protein repeats: structures, functions, and evolution. J Struct Biol. 2001 May-Jun;134(2-3):117-31.

Baker RT, Tobias JW, Varshavsky A. (1992) Ubiquitin-specific proteases of Saccharomyces cerevisiae. Cloning of UBP2 and UBP3, and functional analysis of the UBP gene family. J Biol Chem. 267(32):23364-75

Bernier-Villamor V, Sampson DA, Matunis MJ, Lima CD. Structural basis for E2-mediated SUMO conjugation revealed by a complex between ubiquitin-conjugating enzyme Ubc9 and RanGAP1. Cell. 2002 Feb 8;108(3):345-56.

Biggins S, Murray AW. The budding yeast protein kinase Ipl1/Aurora allows the absence of tension to activate the spindle checkpoint. 2001. Genes Dev. 15:3118–3129.

Bouck D, Bloom K. The role of centromere-binding factor 3 (CBF3) in spindle stability, cytokinesis, and kinetochore attachment. Biochem Cell Biol. 2005 Dec;83(6):696-702.

Bratman, SV and Chang, F. Stabilization of overlapping microtubules by fission yeast CLASP. Dev Cell. 2007 Dec;13(6):812-27.

Cantin GT, Shock TR, Park SK, Madhani HD, Yates JR 3rd. Optimizing TiO2-based phosphopeptide enrichment for automated multidimensional liquid chromatography coupled to tandem mass spectrometry. Anal Chem. 2007 Jun 15;79(12):4666-73. Epub 2007 May 25.

Chan CS and Botstein D. Isolation and characterization of chromosome-gain and increase-in-ploidy mutants in yeast. Genetics. 1993 Nov;135(3):677-91.

Charrasse S, Schroeder M, Gauthier-Rouviere C, Ango F, Cassimeris L, Gard DL, Larroque C. The TOGp protein is a new human microtubule-associated protein homologous to the Xenopus XMAP215. J Cell Sci. 1998 May;111 (Pt 10):1371-83.

Cheeseman IM, Brew C, Wolyniak M, Desai A, Anderson S, Muster N, Yates JR, Huffaker TC, Drubin DG, and Barnes G. Implication of a novel multiprotein Dam1p complex in outer kinetochore function. 2001. J Cell Biol. 155:1137–1146.

Cheeseman IM, Desai A. Molecular architecture of the kinetochore-microtubule interface. Nat Rev Mol Cell Biol. 2008 Jan;9(1):33-46.

Chen Y, Beck A, Davenport C, Chen Y, Shattuck D, Tavtigian SV. Characterization of TRZ1, a yeast homolog of the human candidate prostate cancer susceptibility gene ELAC2 encoding tRNase Z. BMC Mol Biol. 2005 May 13;6(1):12.

Chiron S, Bobkova A, Zhou H, Yaffe MP. CLASP regulates mitochondrial distribution in Schizosaccharomyces pombe. J Cell Biol. 2008 Jul 14;182(1):41-9.

Ciosk R, Zachariae W, Michaelis C, Shevchenko A, Mann M, Nasmyth K. An ESP1/PDS1 complex regulates loss of sister chromatid cohesion at the metaphase to anaphase transition in yeast. Cell. 1998 Jun 12;93(6):1067-76.

Córdova NJ, Ermentrout B, Oster GF. Dynamics of single-motor molecules: the thermal ratchet model. Proc Natl Acad Sci U S A. 1992 Jan 1;89(1):339-43.

Crasta K, Huang P, Morgan G, Winey M, Surana U: Cdk1 regulates centrosome separation by restraining proteolysis of microtubule-associated proteins. Embo J 2006, 25(11):2551-2563.

Crasta K, Surana U. Disjunction of conjoined twins: Cdk1, Cdh1 and separation of centrosomes. Cell Div. 2006 Jun 22;1:12.

D'Amours D, Amon A. At the interface between signaling and executing anaphase--Cdc14 and the FEAR network. Genes Dev. 2004 Nov 1;18(21):2581-95.

Dasso M. Emerging roles of the SUMO pathway in mitosis. Cell Div. 2008 Jan 24;3:5.

De Wulf P, Montani F, Visintin R. Protein phosphatases take the mitotic stage. Curr Opin Cell Biol. 2009 Dec;21(6):806-15.

Denison C, Rudner AD, Gerber SA, Bakalarski CE, Moazed D, Gygi SP. A proteomic strategy for gaining insights into protein sumoylation in yeast. Mol Cell Proteomics. 2005 Mar;4(3):246-54.

Erickson HP. Size and shape of protein molecules at the nanometer level determined by sedimentation, gel filtration, and electron microscopy. Biol Proced Online. 2009 May 15;11:32-51.

Euteneuer U, McIntosh JR. Structural polarity of kinetochore microtubules in PtK1 cells. J Cell Biol. 1981 May;89(2):338-45.

Galjart N. CLIPs and CLASPs and cellular dynamics. Nat Rev Mol Cell Biol. 2005 Jun;6(6):487-98.

Gareau JR, Lima CD. The SUMO pathway: emerging mechanisms that shape specificity, conjugation and recognition. Nat Rev Mol Cell Biol. 2010 Dec;11(12):861-71.

Ghaemmaghami S, Huh WK, Bower K, Howson RW, Belle A, Dephoure N, O'Shea EK, Weissman JS. Global analysis of protein expression in yeast. Nature. 2003 Oct. 16;425(6959):737-41.

Gorbsky GJ, Sammak PJ, Borisy GG. Microtubule dynamics and chromosome motion visualized in living anaphase cells. J Cell Biol. 1988 Apr;106(4):1185-92.

Hannak E, Heald R. Xorbit/CLASP links dynamic microtubules to chromosomes in the Xenopus meiotic spindle. J Cell Biol. 2006 Jan 2;172(1):19-25.

Hannich JT, Lewis A, Kroetz MB, Li SJ, Heide H, Emili A, Hochstrasser M. Defining the SUMO-modified proteome by multiple approaches in Saccharomyces cerevisiae. J Biol Chem. 2005 Feb 11;280(6):4102-10.

Hardwick KG, Weiss E, Luca FC, Winey M, Murray AW. Activation of the budding yeast spindle assembly checkpoint without mitotic spindle disruption. Science. 1996 Aug 16;273(5277):953-6.

Havens KA, Gardner MK, Kamieniecki RJ, Dresser ME, Dawson DS. Slk19p of Saccharomyces cerevisiae regulates anaphase spindle dynamics through two independent mechanisms. Genetics. 2010 Dec;186(4):1247-60.

Hoyt MA, He L, Loo KK, Saunders WS: Two Saccharomyces cerevisiae kinesin-related gene products required for mitotic spindle assembly. J Cell Biol 1992, 118:109-120.

Inoue YH, do Carmo Avides M, Shiraki M, Deak P, Yamaguchi M, Nishimoto Y, Matsukage A, Glover DM. Orbit, a novel microtubule-associated protein essential for mitosis in Drosophila melanogaster. J Cell Biol. 2000 Apr 3;149(1):153-66.

James P, Halladay J, Craig EA. Genomic libraries and a host strain designed for highly efficient two-hybrid selection in yeast. Genetics. 1996 Dec;144(4):1425-36.

Jaspersen SL, Morgan DO. Cdc14 activates cdc15 to promote mitotic exit in budding yeast. Curr Biol. 2000 May 18;10(10):615-8.

Jin F, Liu H, Liang F, Rizkallah R, Hurt MM, Wang Y. Temporal control of the dephosphorylation of Cdk substrates by mitotic exit pathways in budding yeast. Proc Natl Acad Sci U S A. 2008 Oct 21;105(42):16177-82.

Johnson ES, Blobel G. Cell cycle-regulated attachment of the ubiquitin-related protein SUMO to the yeast septins. J Cell Biol. 1999 Nov 29;147(5):981-94.

Kahana JA, Schnapp BJ, Silver PA. Kinetics of spindle pole body separation in budding yeast. Proc Natl Acad Sci U S A. 1995 Oct 10;92(21):9707-11.

Kang J, Cheeseman IM, Kallstrom G, Velmurugan S, Barnes G, Chan CS. Functional cooperation of Dam1, Ipl1, and the inner centromere protein (INCENP)-related protein Sli15 during chromosome segregation. J Cell Biol. 2001 Nov 26;155(5):763-74.

Kawashima SA, Yamagishi Y, Honda T, Ishiguro K, Watanabe Y. Phosphorylation of H2A by Bub1 prevents chromosomal instability through localizing shugoshin. Science. 2010 Jan 8;327(5962):172-7.

Kemmler S, Stach M, Knapp M, Ortiz J, Pfannstiel J, Ruppert T, Lechner J. Mimicking Ndc80 phosphorylation triggers spindle assembly checkpoint signalling. EMBO J. 2009 Apr 22;28(8):1099-110.

Khmelinskii A, Lawrence C, Roostalu J, Schiebel E. Cdc14-regulated midzone assembly controls anaphase B. J Cell Biol. 2007 Jun 18;177(6):981-93.

Khmelinskii A, Schiebel E. Assembling the spindle midzone in the right place at the right time. Cell Cycle. 2008 Feb 1;7(3):283-6.

Khmelinskii A, Roostalu J, Roque H, Antony C, Schiebel E. Phosphorylation-dependent protein interactions at the spindle midzone mediate cell cycle regulation of spindle elongation. Dev Cell. 2009 Aug;17(2):244-56.

Kim JH, Kang JS, Chan CS. Sli15 associates with the ipl1 protein kinase to promote proper chromosome segregation in Saccharomyces cerevisiae. J Cell Biol. 1999 Jun 28;145(7):1381-94.

Kline-Smith SL, Walczak CE. Mitotic spindle assembly and chromosome segregation: refocusing on microtubule dynamics. Mol Cell. 2004 Aug 13;15(3):317-27.

König C, Maekawa H, Schiebel E. Mutual regulation of cyclin-dependent kinase and the mitotic exit network. J Cell Biol. 2010 Feb 8;188(3):351-68.

Kotwaliwale CV, Frei SB, Stern BM, Biggins S. A Pathway Containing the Ipl1/Aurora

Protein Kinase and the Spindle Midzone Protein Ase1 Regulates Yeast Spindle Assembly. Dev Cell. 2007 Sept;13:433.

Lansbergen G, Grigoriev I, Mimori-Kiyosue Y, Ohtsuka T, Higa S, Kitajima I, Demmers J, Galjart N, Houtsmuller AB, Grosveld F, Akhmanova A. CLASPs attach microtubule plus ends to the cell cortex through a complex with LL5beta. Dev Cell. 2006 Jul;11(1):21-32.

Lauzé E, Stoelcker B, Luca FC, Weiss E, Schutz AR, Winey M. Yeast spindle pole body duplication gene MPS1 encodes an essential dual specificity protein kinase. EMBO J. 1995 Apr 18;14(8):1655-63.

Lee SE, Frenz LM, Wells NJ, Johnson AL, Johnston LH. Order of function of the budding-yeast mitotic exit-network proteins Tem1, Cdc15, Mob1, Dbf2, and Cdc5. Curr Biol. 2001 May 15;11(10):784-8.

Lee KS, Park JE, Asano S, Park CJ. Yeast polo-like kinases: functionally conserved multitask mitotic regulators. Oncogene. 2005 Jan 10;24(2):217-29. Review.

Leisner C, Kammerer D, Denoth A, Britschi M, Barral Y, Liakopoulos D. Regulation of mitotic spindle asymmetry by SUMO and the spindle-assembly checkpoint in yeast. Curr Biol. 2008 Aug 26;18(16):1249-55.

Lemos CL, Sampaio P, Maiato H, Costa M, Omel'yanchuk LV, Liberal V, Sunkel CE. Mast, a conserved microtubule-associated protein required for bipolar mitotic spindle organization. EMBO J. 2000 Jul 17;19(14):3668-82.

Li SJ, Hochstrasser M. The yeast ULP2 (SMT4) gene encodes a novel protease specific for the ubiquitin-like Smt3 protein. Mol Cell Biol. 2000 Apr;20(7):2367-77.

Li SJ, Hochstrasser M. The Ulp1 SUMO isopeptidase: distinct domains required for viability, nuclear envelope localization, and substrate specificity. J Cell Biol. 2003 Mar 31;160(7):1069-81.

Link, A.J., J. Eng, D.M. Schieltz, E. Carmack, G.J. Mize, D.R. Morris, B.M. Garvik, and J.R. Yates, III. Direct analysis of protein complexes using mass spectrometry. Nat. Biotechnol. 1999. 17:676–682.

Liu F, Walters KJ. Multitasking with ubiquitin through multivalent interactions. Trends Biochem Sci. 2010 Jun;35(6):352-60.

Longtine MS, McKenzie A 3rd, Demarini DJ, Shah NG, Wach A, Brachat A, Philippsen P, Pringle JR. Additional modules for versatile and economical PCR-based gene deletion and modification in Saccharomyces cerevisiae. Yeast. 1998 Jul;14(10):953-61.

Lopez-Fanarraga M, Avila J, Guasch A, Coll M, Zabala JC. Review: postchaperonin tubulin folding cofactors and their role in microtubule dynamics. J Struct Biol. 2001 Aug;135(2):219-29.

Ma L, McQueen J, Cuschieri L, Vogel J, Measday V. Spc24 and Stu2 promote spindle integrity when DNA replication is stalled. Mol Biol Cell. 2007 Aug;18(8):2805-16.

Maiato H, Khodjakov A, Rieder CL. Drosophila CLASP is required for the incorporation of microtubule subunits into fluxing kinetochore fibres. Nat Cell Biol. 2005 Jan;7(1):42-7.

Maiato H, Khodjakov A, Rieder CL. Drosophila CLASP is required for the incorporation of microtubule subunits into fluxing kinetochore fibres. Nat Cell Biol. 2005 Jan;7(1):42-7.

Mannen H, Tseng HM, Cho CL, Li SS. Cloning and expression of human homolog HSMT3 to yeast SMT3 suppressor of MIF2 mutations in a centromere protein gene. Biochem Biophys Res Commun. 1996 May 6;222(1):178-80.

Manzoni R, Montani F, Visintin C, Caudron F, Ciliberto A, Visintin R. Oscillations in Cdc14 release and sequestration reveal a circuit underlying mitotic exit. J Cell Biol. 2010 Jul 26;190(2):209-22.

Matangkasombut O, Buratowski RM, Swilling NW, Buratowski S. Bromodomain factor 1 corresponds to a missing piece of yeast TFIID. Genes Dev. 2000 Apr 15;14(8):951-62.

Michaelis C, Ciosk R, Nasmyth K. Cohesins: chromosomal proteins that prevent premature separation of sister chromatids. Cell. 1997 Oct 3;91(1):35-45.

Mimori-Kiyosue Y, Grigoriev I, Lansbergen G, Sasaki H, Matsui C, Severin F, Galjart N, Grosveld F, Vorobjev I, Tsukita S, Akhmanova A. CLASP1 and CLASP2 bind to EB1 and regulate microtubule plus-end dynamics at the cell cortex. J Cell Biol. 2005 Jan 3;168(1):141-53.

Mohl DA, Huddleston MJ, Collingwood TS, Annan RS, Deshaies RJ. Dbf2-Mob1 drives relocalization of protein phosphatase Cdc14 to the cytoplasm during exit from mitosis. J Cell Biol. 2009 Feb 23;184(4):527-39.

Montpetit B, Hazbun TR, Fields S, Hieter P. Sumoylation of the budding yeast kinetochore protein Ndc10 is required for Ndc10 spindle localization and regulation of anaphase spindle elongation. J Cell Biol. 2006 Aug 28;174(5):653-63.

Müller S, Hoege C, Pyrowolakis G, Jentsch S. SUMO, ubiquitin's mysterious cousin. Nat Rev Mol Cell Biol. 2001 Mar;2(3):202-10.

Musacchio A, Hardwick KG. The spindle checkpoint: structural insights into dynamic signalling. Nat Rev Mol Cell Biol. 2002 Oct;3(10):731-41.

Ohkura H, Garcia MA, Toda T. Dis1/TOG universal microtubule adaptors - one MAP for all? J Cell Sci. 2001 Nov;114(Pt 21):3805-12.

Ortiz J, Funk C, Schäfer A, Lechner J. Stu1 inversely regulates kinetochore capture and spindle stability. Genes Dev. 2009 Dec 1;23(23):2778-91.

Pasqualone, D and Huffaker TC. STU1, a suppressor of a beta-tubulin mutation, encodes a novel and essential component of the yeast mitotic spindle. J Cell Biol. 1994 Dec;127(6 Pt 2):1973-84.

Pereira G and Schiebel E. Separase regulates INCENP-Aurora B anaphase spindle function through Cdc14. Science. 2003 Dec 19;302(5653):2120-4.

Queralt E, Uhlmann F. Cdk-counteracting phosphatases unlock mitotic exit. Curr Opin Cell Biol. 2008 Dec;20(6):661-8.

Rahal R, Amon A. The Polo-like kinase Cdc5 interacts with FEAR network components and Cdc14. Cell Cycle. 2008 Oct;7(20):3262-72.

Reis R, Feijão T, Gouveia S, Pereira AJ, Matos I, Sampaio P, Maiato H, Sunkel CE. Dynein and mast/orbit/CLASP have antagonistic roles in regulating kinetochore-microtubule plus-end dynamics. J Cell Sci. 2009 Jul 15;122(Pt 14):2543-53.

Roberts BT, Farr KA, Hoyt MA. The Saccharomyces cerevisiae checkpoint gene BUB1 encodes a novel protein kinase. Mol Cell Biol. 1994 Dec;14(12):8282-91.

Rodal AA, Duncan M, Drubin D. Purification of glutathione S-transferase fusion proteins from yeast. Methods Enzymol. 2002;351:168-72.

Sandall S, Severin F, McLoed IX, Yates JR 3rd, Oegema K, Hyman A, Desai A. A Bir1-Sli15 complex connects centromeres to microtubules and is required to sense kinetochore tension. Cell. 2006 Dec 15;127(6):1179-91.

Saunders WS, Koshland D, Eshel D, Gibbons IR, Hoyt MA. Saccharomyces cerevisiae kinesin- and dynein-related proteins required for anaphase chromosome segregation. 1995. J Cell Biol. 128(4):617-24.

Saunders W, Lengyel V, Hoyt MA: Mitotic spindle function in Saccharomyces cerevisiae requires a balance between different types of kinesin-related motors. Mol Biol Cell 1997, 8:1025-1033.

Schiestl RH, Gietz RD. High efficiency transformation of intact yeast cells using single stranded nucleic acids as a carrier. Curr Genet. 1989 Dec;16(5-6):339-46.

Schuyler SC, Liu JY, Pellman D. The molecular function of Ase1p: evidence for a MAP-dependent midzone-specific spindle matrix. J Cell Biol. 2003 Feb 17;160(4):517-28.

Schweitzer B, Philippsen P. CDC15, an essential cell cycle gene in Saccharomyces cerevisiae, encodes a protein kinase domain. Yeast. 1991 Apr;7(3):265-73.

Seufert W, Futcher B, Jentsch S. Role of a ubiquitin-conjugating enzyme in degradation of S- and M-phase cyclins. Nature. 1995 Jan 5;373(6509):78-81.

Shimogawa MM, Graczyk B, Gardner MK, Francis SE, White EA, Ess M, Molk JN, Ruse C, Niessen S, Yates JR 3rd, Muller EG, Bloom K, Odde DJ, Davis TN. Mps1 phosphorylation of Dam1 couples kinetochores to microtubule plus ends at metaphase. Curr Biol. 2006 Aug 8;16(15):1489-501.

Shirayama M, Tóth A, Gálová M, Nasmyth K. APC(Cdc20) promotes exit from mitosis by destroying the anaphase inhibitor Pds1 and cyclin Clb5. Nature. 1999 Nov 11;402(6758):203-7.

Shou W, Seol JH, Shevchenko A, Baskerville C, Moazed D, Chen ZW, Jang J, Shevchenko A, Charbonneau H, Deshaies RJ. Exit from mitosis is triggered by Tem1-dependent release of the protein phosphatase Cdc14 from nucleolar RENT complex. Cell. 1999 Apr 16;97(2):233-44.

Slep, KC. The role of TOG domains in microtubule plus end dynamics. Biochem Soc Trans. 2009 Oct;37(Pt 5):1002-6.

Solinger JA, Pascolini D, Heyer WD. Active-site mutations in the Xrn1p exoribonuclease of Saccharomyces cerevisiae reveal a specific role in meiosis. Mol Cell Biol. 1999 Sep;19(9):5930-42.

Stegmeier F, Amon A. Closing mitosis: the functions of the Cdc14 phosphatase and its regulation. Annu Rev Genet. 2004;38:203-32.

Strawn LA, True HL. Deletion of RNQ1 gene reveals novel functional relationship between divergently transcribed Bik1p/CLIP-170 and Sfi1p in spindle pole body separation. Curr Genet. 2006 Dec;50(6):347-66.

Su LK, Burrell M, Hill DE, Gyuris J, Brent R, Wiltshire R, Trent J, Vogelstein B, Kinzler KW. APC binds to the novel protein EB1. Cancer Res. 1995 Jul 15;55(14):2972-7.

Sullivan M, Lehane C, Uhlmann F. Orchestrating anaphase and mitotic exit: separase cleavage and localization of Slk19. Nat Cell Biol. 2001 Sep;3(9):771-7.

Sullivan M, Morgan DO. Finishing mitosis, one step at a time. Nat Rev Mol Cell Biol. 2007 Nov;8(11):894-903.

Tanaka K, Mukae N, Dewar H, van Breugel M, James EK, Prescott AR, Antony C, Tanaka TU. Molecular mechanisms of kinetochore capture by spindle microtubules. Nature. 2005 434:987-994.

Tanaka TU, Rachidi N, Janke C, Pereira G, Galova M, Schiebel E, Stark MJ, and Nasmyth K. Evidence that the Ipl1–Sli15 (Aurora kinase-INCENP) complex promotes chromosome bi-orientation by altering kinetochore-spindle pole connections. 2002. Cell. 108:317–329.

Tang Z, Shu H, Oncel D, Chen S, Yu H (2004) Phosphorylation of Cdc20 by Bub1 provides a catalytic mechanism for APC/C inhibition by the spindle checkpoint. Mol. Cell. 16:387–397.

Visintin R, Craig K, Hwang ES, Prinz S, Tyers M, Amon A. 1998. The phosphatase Cdc14 triggers mitotic exit by reversal of Cdk-dependent phosphorylation. Mol. Cell. 2:709–18

Wei RR, Sorger PK, Harrison SC. Molecular organization of the Ndc80 complex, an essential kinetochore component. Proc Natl Acad Sci U S A. 2005 Apr 12;102(15):5363-7.

Wei RR, Al-Bassam J, Harrison SC. The Ndc80/HEC1 complex is a contact point for kinetochore–microtubule attachment. Nat Struct Mol Biol. 2007. 14:54–59.

Westermann S, Avila-Sakar A, Wang H-W, Niederstrasser H, Wong J, Drubin DG, Nogales E, Barnes G. Formation of a dynamic kinetochore-microtubule interface through assembly of the Dam1 ring complex. Mol Cell. 2005 17:277–290.

Westermann S, Drubin DG, Barnes G. Structures and functions of yeast kinetochore complexes. Annu Rev Biochem. 2007;76:563-91.

Wigge PA, Kilmartin JV. The Ndc80p complex from Saccharomyces cerevisiae contains conserved centromere components and has a function in chromosome segregation. J Cell Biol. 2001 Jan 22;152(2):349-60.

Winey M, Mamay CL, O'Toole ET, Mastronarde DN, Giddings TH Jr, McDonald KL, McIntosh JR. Three-dimensional ultrastructural analysis of the Saccharomyces cerevisiae mitotic spindle. J Cell Biol. 1995 Jun;129(6):1601-15.

Winey M, O'Toole ET. The spindle cycle in budding yeast. Nat Cell Biol. 2001 Jan;3(1):E23-7.

Wohlschlegel JA, Johnson ES, Reed SI, Yates JR 3rd. Global analysis of protein sumoylation in Saccharomyces cerevisiae. J Biol Chem. 2004 Oct 29;279(44):45662-8.

Woodbury EL, Morgan DO. Cdk and APC activities limit the spindle-stabilizing function of Fin1 to anaphase. Nat Cell Biol. 2007 Jan;9(1):106-12.

Wu X, Xiang X, Hammer JA 3rd. Motor proteins at the microtubule plus-end. Trends Cell Biol. 2006 Mar;16(3):135-43.

Wykoff DD, O'Shea EK. Identification of sumoylated proteins by systematic immunoprecipitation of the budding yeast proteome. Mol Cell Proteomics. 2005 Jan;4(1):73-83.

Xirodimas DP. Novel substrates and functions for the ubiquitin-like molecule NEDD8. Biochem Soc Trans. 2008 Oct;36(Pt 5):802-6.

Yin H, You L, Pasqualone D, Kopski KM, Huffaker, TC. Stu1p is physically associated with b-tubulin and is required for structural integrity of the mitotic spindle. Mol Biol Cell. 2002 Jun;13(6):1881-92.

Yunus AA, Lima CD. Lysine activation and functional analysis of E2-mediated conjugation in the SUMO pathway. Nat Struct Mol Biol. 2006 Jun;13(6):491-9.

Zeng X, Kahana JA, Silver PA, Morphew MK, McIntosh JR, Fitch IT, Carbon J, Saunders WS. Slk19p is a centromere protein that functions to stabilize mitotic spindles. J Cell Biol. 1999 Jul 26;146(2):415-25.

Zhang T, Lim HH, Cheng CS, Surana U. Deficiency of centromere-associated protein Slk19 causes premature nuclear migration and loss of centromeric elasticity. J Cell Sci. 2006 Feb 1;119(Pt 3):519-31.

Zhou W, Ryan JJ, Zhou H. Global analyses of sumoylated proteins in Saccharomyces cerevisiae. Induction of protein sumoylation by cellular stresses. J Biol Chem. 2004 Jul 30;279(31):32262-8. Epub 2004 May 27.

Zich J, Hardwick KG. Getting down to the phosphorylated 'nuts and bolts' of spindle checkpoint signalling. Trends Biochem Sci. 2010 Jan;35(1):18-27.

Appendix: Supplemental Tables

Supplemental Table 1. Proteins identified in mass spectrometric analysis of Slk19-TAP purification

Protein name	# peptides detected	Sequence coverage (%)	Protein name	# peptides detected	Sequence coverage (%)
Slk19	3129	88.6	Nrp1	2	3.3
Tef1/2	206	42.6	Sld3	2	3.3
Act1	77	40.3	Tos2	2	3.2
Cpr1	3	24.2	Bye1	2	3.2
Hyp2	19	23.6	Utp7	2	3.2
Scw10	6	16.5	Gus1	6	3.1
Vma2	9	16.2	Bdp1	2	3.0
Cnl1	2	14.8	Mms4	6	2.9
Smc3*	8	12.6	Atg7	2	2.9
Cof1	3	11.9	Pab1	2	2.9
Gsp1/2*	15	11.4	Vps30	3	2.9
Ivy1	4	9.5	Rok1	2	2.8
Tda2	2	9.5	Skn1	2	2.7
Tfb3	4	9.3	Sly1	2	2.7
Hrp1	2	7.7	Zpr1	2	2.7
Rep1/2	11	7.6	Sub2	2	2.7
Ola1	3	7.6	Nup188	2	2.6
Pho88	2	7.4	Nab3	2	2.6
Bmh1/2	3	7.3	Ent2	2	2.6
Scj1	4	7.2	Vps27	2	2.6
Rvs161	3	7.2	Tod6	7	2.5
Hpa2	2	7.1	Kem1	4	2.4
YHR020W	5	6.5	Mcm6	2	2.4
Pac10	2	6.5	Pdc2	3	2.4
YMR315W	2	6.3	Elp2	2	2.3
Otu2	2	6.2	Sov4	24	2.2
Cct8	2	5.5	Doa1	2	2.2
Dam1*	3	5.5	Dbp2	2	2.2
Osh3	2	5.4	Sec5	2	2.1
Cax4	3	5.4	YGL140C	2	2.0
Ngg1	4	5.3	Vma13	2	1.9
Mph1	2	5.2	Sin3	2	1.8
YBR242W	4	5.0	Pan1	2	1.8
Sae2	2	4.9	Vps72	3	1.8
Mcm3	2	4.5	Mrc1	12	1.7
Tif5	2	4.4	Pho90	3	1.7
Arc1	2	4.3	Far11	3	1.6
Frs2	2	4.2	Arg81	2	1.6
Yhi9	2	3.7	Cat8	15	1.3
Tfp1	8	3.6	Sac3	2	1.2
Npr2	2	3.6	Spc110*	2	1.2
YEL023C	2	3.5	YFR016C	2	1.1
Yef3	5	3.4	Ecm21	2	1.1
Agp2	6	3.4	Num1*	2	1.0
YJR061W	2	3.3	Rpo31	11	0.8
Eft1/2	3	3.3	Taf2	2	0.8

List of proteins that were identified as multiple peptides in a Slk19-TAP purification and mass spectrometric analysis. Certain classes of proteins that are unlikely to be true interacting proteins were not included in this list (ribosomal and ribosome-associated proteins, metabolic enzymes, heat shock proteins, dubious open reading frames and mitochondrial proteins). Proteins marked with "*" indicate interesting interacting proteins with regard to the known functions of Slk19 (e.g., mitotic proteins, chromatid cohesion proteins and kinetochore-associated proteins).

Supplemental Table 2. Proteins identified by single peptides in mass spectrometric analysis of Slk19-TAP purification

Protein name	# peptides detected	Sequence coverage (%)	Protein name	# peptides detected	Sequence coverage (%)
Gar1	1	20.0	Arp4	1	2.7
Irc4	1	15.6	Kre2	1	2.7
Mms2*	1	15.3	Gto3	1	2.7
Spc25*	1	14.9	Ybt1	1	2.6
Syf2	1	13.5	Rom1	1	2.6
YCL075W	1	12.3	Mcm5	1	2.6
Arf3	1	11.5	Kar3*	1	2.6
Tvp23	1	11.1	Mtc4	1	2.6
Smt3*	1	10.9	Mlh2	1	2.6
Otu1	1	10.6	Trm1	1	2.6
Sds3	1	8.3	Tub2*	1	2.6
Spc29*	1	8.3	Rgt1	1	2.5
Rpn13	1	8.3	Nup2	1	2.5
Pex15	1	8.1	Bdf2	1	2.5
YOR214C	1	8.1	Yku80	1	2.5
Ccw14	1	8.0	Mum3	1	2.5
Eco1*	1	7.8	Gda1	1	2.5
YGR079W	1	7.6	Gef1	1	2.4
Lcl2	1	7.6	Sgm1	1	2.4
Csl4	1	7.6	YKR017C	1	2.4
Egd2	1	7.5	Stp2	1	2.4
Aim20	1	7.4	Ses1	1	2.4
Tif35	1	7.3	Sps22	1	2.4
Dcw1	1	7.1	Ptc3	1	2.4
Yap3	1	7.0	Arp3	1	2.4
Mgt1*	1	6.9	Tps2	1	2.3
Bop3	1	6.8	Sgd1	1	2.3
Cup2	1	6.7	Upc2	1	2.3
Ysc84	1	6.6	Jip4	1	2.3
Ett1	1	6.6	Red1	1	2.3
Cdc73	1	6.6	Cla4	1	2.3
Rpb3	1	6.6	Rfx1	1	2.3
Hho1*	1	6.6	Fra1	1	2.3
Ino4	1	6.6	Bdf1	1	2.3
YLR030W	1	6.5	Aip1	1	2.3
Smk1	1	6.4	Atp2	1	2.3
Air1	1	6.4	Tif34	1	2.3
Sua5	1	6.3	Taf1	1	2.2
YJL107C	1	6.2	Crt10	1	2.2

Cwc2	1	6.2	Tif4631	1	2.2
Pno1	1	6.2	Ist2	1	2.2
YER079W	1	6.2	YPL150W	1	2.2
YGR053C	1	6.0	Epl1	1	2.2
Naf1	1	5.9	Sec6	1	2.2
Pst1	1	5.9	Dbp7	1	2.2
Reg2*	1	5.9	Asi1	1	2.2
YGL081W	1	5.9	Alg9	1	2.2
Gzf3	1	5.8	Seg2	1	2.1
Pho11/12	1	5.8	Prp16	1	2.1
Prm6	1	5.7	Pep3	1	2.1
Dog1/2	1	5.7	Nat1	1	2.1
Sts1	1	5.6	Dsl1	1	2.1
Yrb1	1	5.5	Prp43	1	2.1
Gcs1	1	5.4	Itr2	1	2.1
YNL010W	1	5.4	Cdh1*	1	2.1
Pex31	1	5.1	Tcp1	1	2.1
Mus81	1	5.1	Brl1	1	2.1
Ssp120	1	5.1	Avo2	1	2.1
Srd1	1	5.0	Yng2	1	2.1
Cdc12*	1	4.9	Mnn4	1	2.0
Yef1	1	4.8	Srs2	1	2.0
Dma1	1	4.8	Pho81	1	2.0
Dat1	1	4.8	Ubp7	1	2.0
YNL181W	1	4.7	Phm7	1	2.0
Paa1	1	4.7	Rck2	1	2.0
YPR148C	1	4.6	Gap1	1	2.0
Pol32	1	4.6	Mih1	1	2.0
Sph1	1	4.5	Pub1	1	2.0
Ypt31/2	1	4.5	Apl3	1	1.9
Ubp6	1	4.4	Rsn1	1	1.9
Cdc123	1	4.4	Cdc13	1	1.9
Sgn1	1	4.4	Ctf4*	1	1.9
YGL039W	1	4.3	Hul4	1	1.9
Sec2	1	4.2	Def1	1	1.9
Slu7	1	4.2	Nup192	1	1.8
Dug3	1	4.2	Spt5	1	1.8
Rpc40	1	4.2	Stb2	1	1.8
Mft1	1	4.1	Sbe22	1	1.8
Tif1/2	1	4.1	Mbp1	1	1.8
Pby1	1	4.0	Mtc5	1	1.7
Swc4	1	4.0	Gpb1	1	1.7
Rtf1	1	3.9	Reb1	1	1.7
Rio1	1	3.9	Hrk1	1	1.7

YKL133C	1	3.9	Haa1	1	1.7
Lsb3	1	3.9	Msh6	1	1.6
Mei4	1	3.9	Ssd1	1	1.6
Err1/2/3	1	3.9	YPL216W	1	1.6
YDR282C	1	3.9	YMR196W	1	1.6
Nvj2	1	3.8	Kap122	1	1.6
San1	1	3.8	Boi2	1	1.6
Ref2	1	3.8	Mcm6	1	1.6
Ysp3	1	3.8	Ndc10*	1	1.6
Sly41	1	3.8	Pif1	1	1.6
Rad61*	1	3.7	YGR130C	1	1.6
Ppt1	1	3.7	Aco2	1	1.6
Clb3*	1	3.7	Dsf2	1	1.6
Gbp2	1	3.7	Pan1	1	1.5
Dse3	1	3.7	Smc6*	1	1.5
Afg2	1	3.6	Ams1	1	1.5
Sam3	1	3.6	Mtr1	1	1.5
Vps17	1	3.6	Sec1	1	1.5
Ssn3	1	3.6	Skg3	1	1.4
Hsv2	1	3.6	Egt2	1	1.4
Yvh1	1	3.6	Prp5	1	1.4
Irc5	1	3.5	Pho84	1	1.4
Psr1	1	3.5	Mms22	1	1.3
Bub3*	1	3.5	Flo1	1	1.3
Vps5	1	3.4	Bub1*	1	1.3
Tpo1	1	3.4	Siz1*	1	1.3
Yhp1	1	3.4	Mot1	1	1.2
YEL025C	1	3.3	Stu1*	1	1.2
Nsp1	1	3.3	Bnr1	1	1.2
Yck2	1	3.3	Ssk22	1	1.2
Rrt12	1	3.3	YOL075C	1	1.2
Arp2	1	3.3	Rpa135	1	1.2
Pig1*	1	3.2	Nmd2	1	1.2
Dbp9	1	3.2	Hbt1	1	1.2
Cct2	1	3.2	Sok1	1	1.2
Tda6	1	3.2	Nip100*	1	1.2
Aim45	1	3.2	Apc1*	1	1.1
Spo22	1	3.1	Pmd1	1	1.1
Exo84	1	3.1	Ecm5	1	1.1
Snu71	1	3.1	Gin4	1	1.1
Rtk1	1	3.1	Rim13	1	1.1
Pap2	1	3.1	Tao3	1	1.0
Ngl2	1	3.1	Sec7	1	1.0
Esc2*	1	3.1	Fsk3	1	1.0

Tex1	1	3.1	Pdr12	1	1.0
Nam7	1	3.0	Mlh1	1	1.0
Arn2	1	3.0	Blm10	1	0.9
Prb1	1	3.0	Mot1	1	0.9
Dbf2*	1	3.0	Ycs4	1	0.9
Eki1	1	3.0	Arp8	1	0.9
Ngl3	1	3.0	Tor2	1	0.8
Mpc54	1	3.0	Sec16	1	0.8
Crp1	1	3.0	Uso1	1	0.8
Cin8*	1	2.9	Mlp2	1	0.8
Plb3	1	2.9	Myo2	1	0.8
Pol4	1	2.9	Pdr10	1	0.8
Rsc8	1	2.9	Tcb3	1	0.8
Bgl2	1	2.9	Cdc39	1	0.8
Psy3	1	2.9	YPR117W	1	0.6
Nha1	1	2.8	Ski3	1	0.6
YMR031C	1	2.8	Ira1	1	0.5
Aim44	1	2.8	Mlp1	1	0.4
Gsm1	1	2.8	Mdn1	1	0.3
Ysw1	1	2.8			
Cog8	1	2.8			
Ltv1	1	2.8			
Cdc24	1	2.7			
Rsp5	1	2.7			
Atg15	1	2.7			
Sas4	1	2.7			

List of proteins that were identified as single peptides in a Slk19-TAP purification and mass spectrometric analysis. Certain classes of proteins that are unlikely to be true interacting proteins were not included in this list (ribosomal and ribosome-associated proteins, metabolic enzymes, heat shock proteins, dubious open reading frames and mitochondrial proteins). Proteins marked with "*" indicate interesting interacting proteins with regard to the known functions of Slk19 (e.g., mitotic proteins, chromatid cohesion proteins and kinetochore-associated proteins).